ELSEVIER

Ore Geology Reviews 18 (2001) 181–209

ORE GEOLOGY REVIEWS

www.elsevier.com/locate/oregeorev

Nature and origin of the Vani manganese deposit, Milos, Greece: an overview

A. Liakopoulos [a], G.P. Glasby [b,*,1], C.T. Papavassiliou [b], J. Boulegue [c]

[a] *Institute of Geology and Mineral Exploration (I.G.M.E.), 70 Messoghion St., 115 27 Athens, Greece*
[b] *Department of Economic Geology and Geochemistry, University of Athens, Panepistimioupoli, Zografou, Athens 157 84, Greece*
[c] *Science de la Terre et Evolution des Milieux Naturels, Case 3000, Université Pierre et Marie Curie, 4, Place Jussieu, F-75252 Paris Cedex 05, France*

Received 2 August 2000; accepted 31 May 2001

Abstract

The Vani manganese deposit is located in the rugged NW sector of Milos Island. It occurs within the Vani volcano-sedimentary basin, which is underlain by dacitic domes and flows of Upper Pliocene age (3.5–2.0 Ma). The end of the emplacement of the dacites was marked by the collapse of the magma chamber, which resulted in a huge pyroclastic episode and the deposition of a thick layer of pyroclastic material within a shallow submarine basin. This pyroclastic material subsequently compacted to form the volcaniclastic sandstone, which became the host for the manganese ore beds which were about 4 m thick in the two sections studied. Hydrothermal fluids penetrated these sandstone horizons via fractures and fissures to produce the manganese deposit. The permeable nature of the sandstone facilitated the retention of the hydrothermal fluids within these layers. This permitted the fluids to cool slowly and deposit the manganese oxides almost quantitatively. Formation of the hydrothermal manganese deposit took place fairly rapidly over a period of several tens of thousands of years at most. Strong tectonic activity resulted in rapid uplift of the area which elevated the deposit above sea level.

Two generations of manganese oxides have been identified within this deposit; the first generation consists of pyrolusite and ramsdellite; the second generation of oxides of the isostructural series cryptomelane–hollandite–coronadite plus hydrohetaerolite characterized by high contents of K, Ba, Pb and Zn, respectively. This sequence is the result of a two-stage process of formation of the manganese-oxide minerals in which a second high-salinity hydrothermal fluid enriched in Ba, Pb and Zn as a result of the dissolution of sulphide minerals remineralized the original manganese-oxide assemblage. It is this two-stage process of formation, which was mainly responsible for the unique characteristics of this deposit. Although formed in a submarine setting, the deposit shows marked differences in mineralogy and composition from known submarine hydrothermal manganese deposits and is most analogous to the epithermal vein deposits of the southwestern United States.

Keywords: Cape Vani; Milos; Manganese deposit; Hydrothermal fluids; Volcaniclastic sandstone

1. Introduction

The island of Milos is located in the central part of the southern Aegean Sea and belongs to the active volcanic region of the Aegean Arc. This arc comprises five volcanic centres (Sousaki, Methana, Mi-

* Corresponding author.
E-mail address: glasby@eqchem.s.u-tokyo.ac.jp (G.P. Glasby).
[1] Address until 30/6/2002: Laboratory for Earthquake Chemistry, University of Tokyo, 7-3-1 Hongo, Bunkyo-ku, Tokyo 113-0033, Japan.

0169-1368/01/$ - see front matter
PII: S0169-1368(01)00029-4

los, Santorini, Nisyros; Fig. 1). Of these, the islands of Methana and Santorini are presently volcanically active, whereas Milos and Nisyros display only hydrothermal activity (gas and fluid emanations), but are potentially volcanically active. Volcanism on Milos dates from 3.5 to 0.08 Ma and the volcanic sequence is overlain by recent alluvial deposits (Fytikas, 1989; Fytikas et al., 1986). Four main cycles of volcanic activity have been distinguished (Fytikas et al., 1986). The oldest volcanic activity is situated in the western part of Milos and took place during the Upper Pliocene (3.5–2.0 Ma). It began with submarine eruptions and the deposition of pyroclastic material followed by subaerial eruptions, mainly lava domes and flows. This phase of volcanism is believed to have been fed by material deep in the continental crust where contamination and fractional crystallization occurred. The dominant rock types at this time were andesites and dacites (Fytikas et al., 1986). Fig. 2 is a neotectonic map of Milos, which outlines the main features of the geology of the island (Papanikolaou et al., 1993).

The tectonic regime along the Aegean Arc has been described by Papazachos and Panagiotopoulos (1993), Papazachos et al., (1993, 2000) and Pavlakis (1993) and the petrogenesis of the volcanic rocks of the arc by Mitropoulos et al., (1987) and Mitropoulos and Tarney (1992). According to Papazachos and Panagiotopoulos (1993), the higher volcanic activity in the eastern volcanic centres of the arc (Santorini, Nisyros) compared to the western volcanic centres (Sousaki, Methana, Milos) reflects the higher rate of extensional crustal deformation in the eastern part of the arc (26 mm year^{-1}) compared to the western part

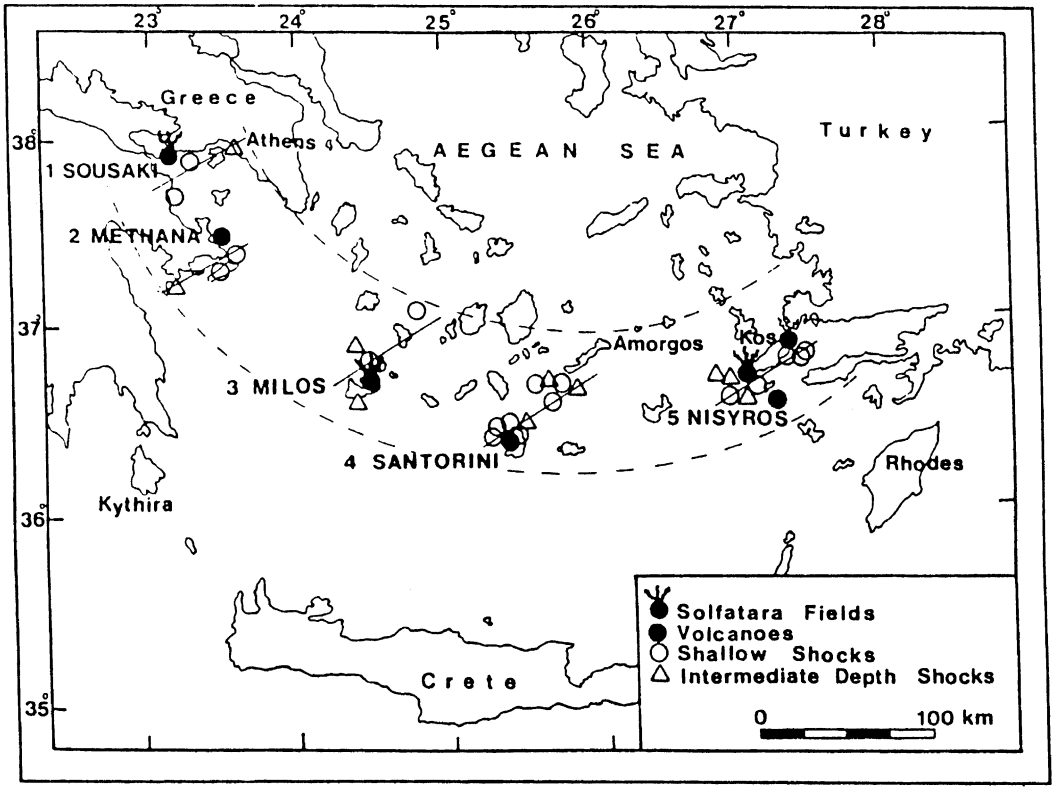

Fig. 1. Simplified map showing the locations of the five volcanic centres, which make up the Aegean Arc. The centres are associated with normal faults trending about N59° (lines) and are marked by frequent earthquakes (circles) and sulphurous volcanic gases (squares) (taken from Papazachos and Panagiotopoulos, 1993).

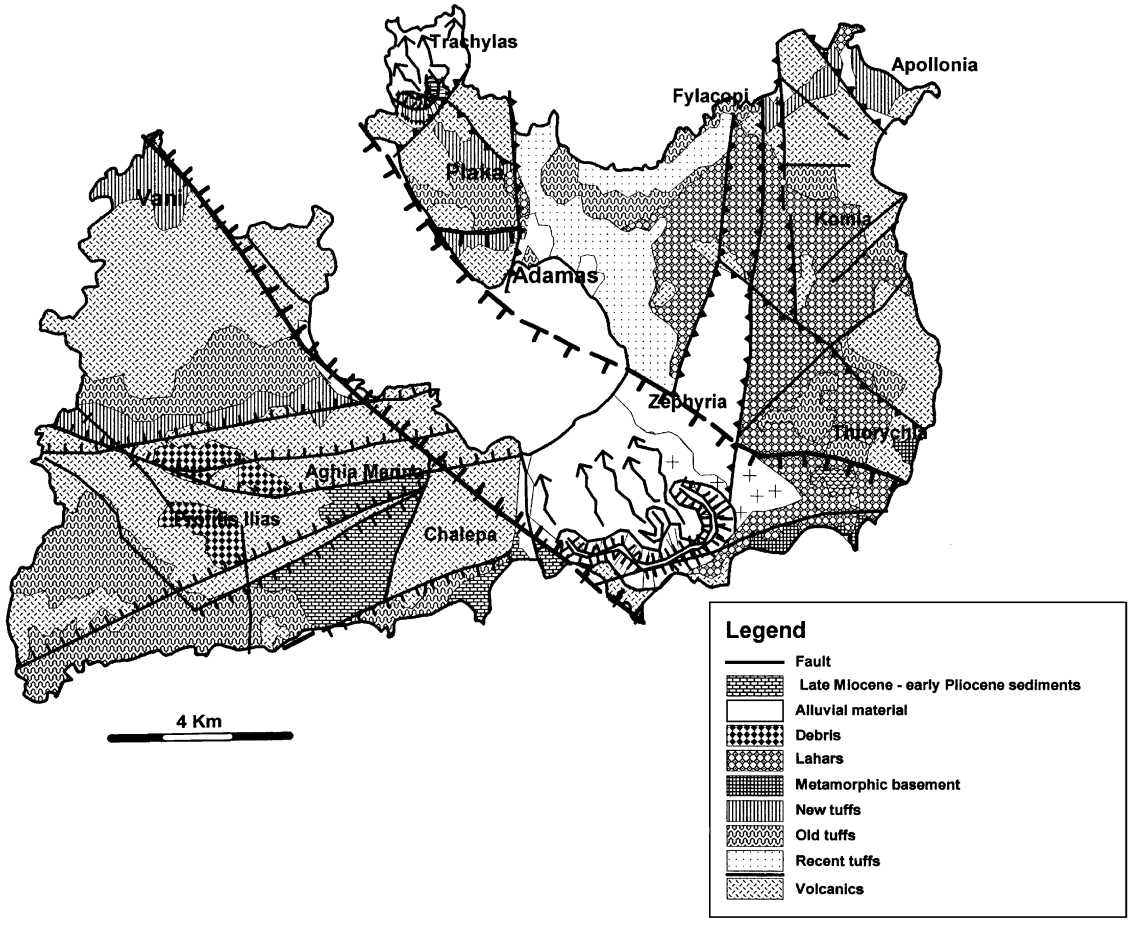

Fig. 2. Simplified geological map of Milos (taken from Papanikolaou et al., 1993). The Vromolimni–Kondaro Fault marks the western boundary of Milos Bay.

of the arc (2 mm year^{-1}). Five normal faults trending about N59° and named after the corresponding volcanic centres appear to control the distribution of volcanic centres and shallow (< 20 km) and intermediate (120–180 km) depth seismicity along the arc (Fig. 1). These faults have had a major influence in controlling the distribution of hydrothermalism along the arc.

Fig. 2 shows the locations of the main NW–SE faults, which have created the active tectonic block which separates western from eastern Milos (Delibasis and Drakopoulos, 1993; Papanikolaou et al., 1993). These faults are intersected in the south by the important E–W fault zone of Aghia Kiriaki (Makropoulos et al., 2000). On Milos, there is a clear relation between seismically activated faults, volcanic activity and hydrothermal phenomena (Papanikolaou et al., 1993; Makropoulos et al., 2000). The extensional stress field on Milos has varied between NE–SW in the Pliocene and NW–SE in the Quaternary (Fytikas, 1989) although the regional stress field was much weaker during the late Pliocene than at present (Mercier, 1981).

The Milos archipelago is the most important volcanic centre in the Aegean Arc in terms of the quantity and variety of volcanic products, explosive volcanic activity and duration of activity (Fytikas et al., 1986). Plio–Quaternary magmatic activity led to the development of a high enthalpy geothermal field on Milos, which is considered to be the most impor-

tant in Greece (Fytikas and Marinelli, 1976). The strong tensional tectonic regime on Milos resulted in extensive faulting, which has stimulated volcanic activity and geothermal fluid circulation, particularly, in the Quaternary (Fytikas, 1989).

The widespread occurrence of fossil and recent hydrothermal activity on Milos as exemplified by the occurrence of hot springs (30–85 °C), fumaroles (98–102 °C), hot grounds (with temperatures of up to 100 °C at depths of 0.3 m below the surface) and phreatic explosions have led to extensive alteration and self-sealing of the volcanic rocks to produce a caprock for the geothermal fluids (Liakopoulos, 1987; Fytikas, 1989; Fytikas et al., 1989). Models for the nature and origin of the convection cell, which forms the deep geothermal reservoir on Milos, have been developed by a number of authors (Liakopoulos, 1987; Liakopoulos and Boulegue, 1987; Liakopoulos et al., 1991; Mendrinos, 1988; Fytikas et al., 1989; Galanopoulos et al., 1991; Pflumio et al., 1993; Minissale et al., 1997).

The intense hydrothermal activity on Milos has resulted in the formation of various hydrothermal minerals, such as alunite, kaolinite, sulphur, barite, galena, manganese and iron oxides, and epithermal gold (Fytikas and Marinelli, 1976; Fytikas and Markopoulos, 1992; Fytikas et al., 1995; Kelepertsis et al., 1990; Liakopoulos, 1991; Plimer, 2000), of which kaolin and barite (as well as perlite and bentonite) are presently being mined (Christidis et al., 1995; Stamatakis et al., 1996; Koukouzas et al., 2000; Plimer, 2000). An extensive exploration programme is now underway to search for epithermal gold (Spartali, 1994; Anonymous, 1999a,b; Plimer, 2000; Kilias et al., 2001). Barite mineralization was considered to have formed as a consequence of

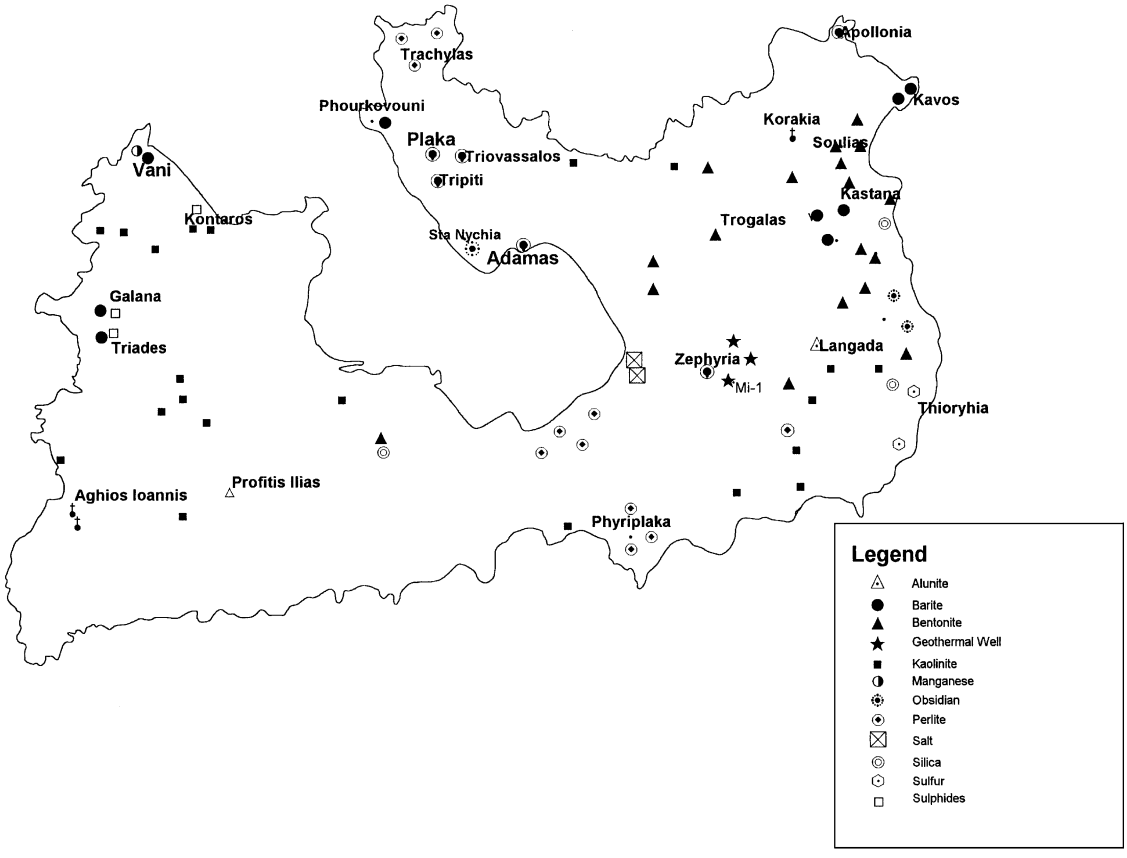

Fig. 3. Locations of the principal industrial mineral deposits on Milos (taken from Liakopoulos, 1987).

Kuroko-type ore deposition (Kalogeropoulos and Mitropoulos, 1983: Hauck, 1984, 1988); however, this idea is no longer accepted. This hydrothermal activity has resulted in Milos being the most mineralized island in Europe with about one-third of its surface area hydrothermally altered. Fig. 3 shows the locations of the principal industrial mineral deposits on the island (Liakopoulos, 1987; Fytikas and Markopoulos, 1992; Stamatakis et al., 1996).

Submarine hydrothermal activity is also well known on Milos, e.g. at Paleohori Bay on the SE coast of Milos (Stüben and Glasby, 1999). Excellent overviews of submarine hydrothermal activity and mineralization in the Mediterranean and Aegean Seas have been presented by Dando et al. (1999, 2000).

From the preceeding comments, it can be seen that Milos is an area of extreme geological interest and worthy of much more detailed investigation. A detailed account of the geological and mining history of the island has recently been published by Plimer (2000).

2. The Vani manganese deposit

2.1. Geological setting

The Vani manganese deposit is located in the area of Cape Vani in the rugged NW sector of the island of Milos about 20 km by road from the port of Adamas. The deposit has been estimated by Hauck (1984) to cover an area in excess of 100,000 m^2 and by Schmidt (1966) an area of 176,000 m^2. It lies proximal to the sea and occurs between 35 m above sea level and an unknown depth below sea level. The deposit is quite small by world standards with reserves estimated to be about 2.1 million tonnes of manganese ore (Glasby et al., 2001). It was mined between 1886 and 1909 and again between 1916 and 1928. Between 1886 and 1909, 220,000 tonnes of ore were recovered.

The Vani manganese deposit is situated within the Vani volcano-sedimentary basin. This basin is underlain by hydrothermally altered dacitic lava domes and flows, which are Upper Pliocene in age (3.5–2.0 Ma) (Fytikas et al., 1986). The overlying volcanic-sedimentary sequence consists of tuffaceous clastic and volcaniclastic deposits, which are lower to middle Pleistocene and were deposited sometime in the period 0.9–0.4 Ma (Papanikolaou et al., 1990).

The manganese oxides at Cape Vani formed as impregnations in a series of volcaniclastic sandstone horizons. The volcaniclastic sandstone occupies a surface area of about 1 km^2 and occurs at the centre of the Vani basin. This basin is made up of highly altered dacites, which belong to Unit II of the Milos volcanostratigraphy (Angelier et al., 1977) (Fig. 4). The basin is now open to the sea on the NW and NE coasts as a result of a system of faults aligned 90° to each other. The assemblage of volcaniclastic sandstone and dacites occupies an area of 11 km^2.

The volcaniclastic sandstone is altered pyroclastic material of Upper Pliocene age. It consist of two units, lower and upper, separated by a thin layer of conglomerates (0–0.3 m thick) composed of pebbles of volcaniclastic sandstone and dacite. The sandstone contains badly preserved fossils of the Lamellibranch family (*Pecten* sp., *Ostrea* sp.), echinoids and brachiopods, which indicates that they were formed in a restricted, shallow marine basin (cf. Fytikas, 1977; I.G.M.R., 1977; Liakopoulos, 1987; Kelepertzis and Kyriakopoulos, 1991; Plimer, 2000).

The shape of the basin is the result of the superposition of a number of faults which can be grouped into three major systems trending: N90°, N315°–320° and N30°, respectively. The superposition of these three fault systems results in a NNW–SSE basin which slopes gently to the NNW.

The manganese mineralization is stratabound in the lower volcaniclastic sandstone unit. Based on exposures from the open-cast mining, it was possible to construct the succession of the formations at two locations (Figs. 5 and 6). However, because of extensive faulting in the area, these profiles cannot be considered to be representative of manganese deposition throughout the entire basin.

The underlying volcaniclastic sandstone is strongly silicified and impregnated by manganese oxides and is composed mainly of K-feldspar, chlorite and sericite. The plagioclases are in the process of sericitization and adularization.

The manganese ore beds in these two sections are about 4 m thick. The manganese oxides form a cement in which K-feldspar is the dominant mineral present.

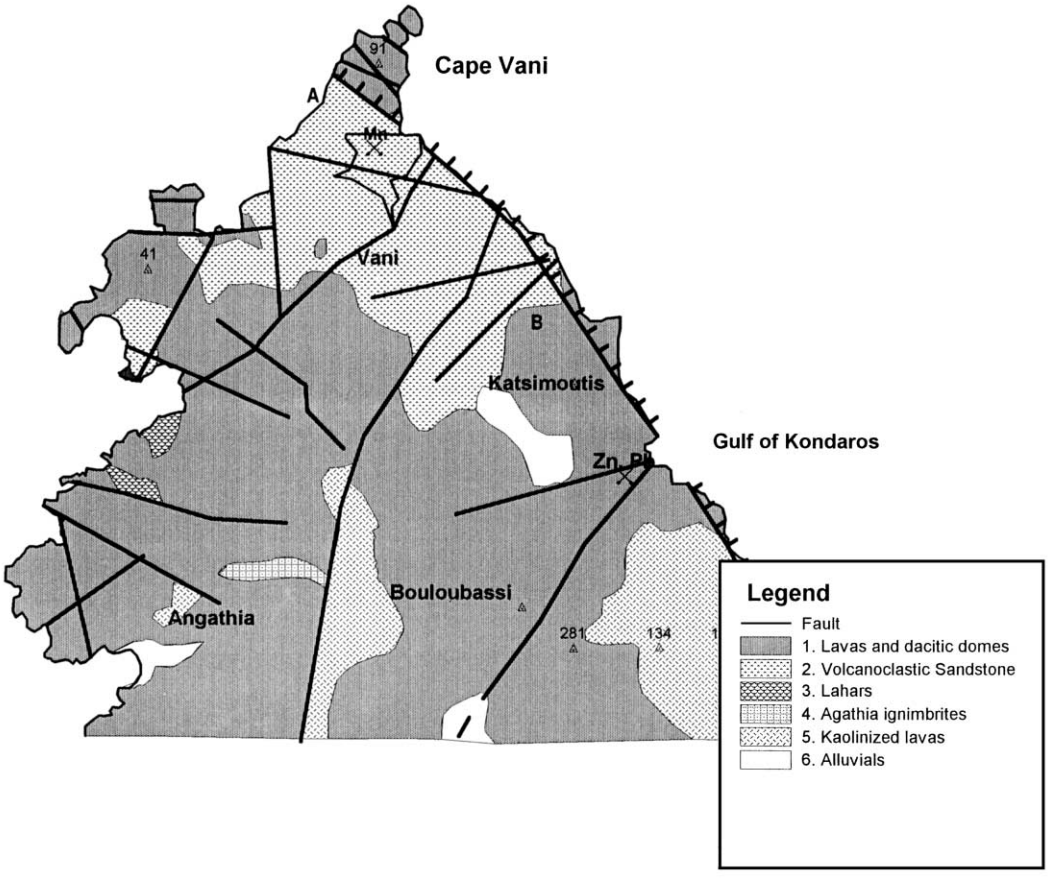

Fig. 4. Geological sketch map of Cape Vani. (1) Lavas and dacitic domes; (2) volcaniclastic sandstone; (3) lahars; (4) Angathias ignimbrites; (5) kaolinized lavas; (6) alluvials; (7) Vani manganese deposit (taken from Liakopoulos, 1987).

The overlying volcaniclastic sandstone comprises two types, a green horizon and a white horizon. Lying immediately above the manganese-oxide layer is a green horizon which varies in thickness from a few cm to 2 m. This horizon is made up of glauconite, K-feldspar and sericite and is easily recognizable in this terrain. Above this lies a white horizon up to 6 m thick, which consists of an assemblage of K-feldspar and oligoclase cemented by a siliceous matrix. The silica is present as amorphous silica, quartz or cristobalite. Arseniosiderite occurs in the white horizon in concentrations in the range 0–15% (based on X-ray diffraction analysis). The places where arseniosiderite occurs are coloured red and are very characteristic of the terrain. This red colouration is due to the presence of iron, which occurs both in the arseniosiderite as well as in the ferruginous matrix. Only small amounts of haematite were identified in this red layer.

Barite occurs in variable amounts throughout the sections. In the mineralized zone, it averages 12.5% and displays evidence of dissolution and replacement by manganese oxides. The manganese deposits are cut by veins of quartz and barite, which post-date the manganese mineralization. These veins are oriented in two principal directions, N320° and N30°.

In fact, information on the Vani manganese deposit in English is relatively sparse. Two of the earliest studies of this deposit focussing mainly on economic aspects were undertaken at the University of Leoben in Austria (Argyropoulos, 1966; Schmidt, 1966) and were briefly summarized by Mack (1977).

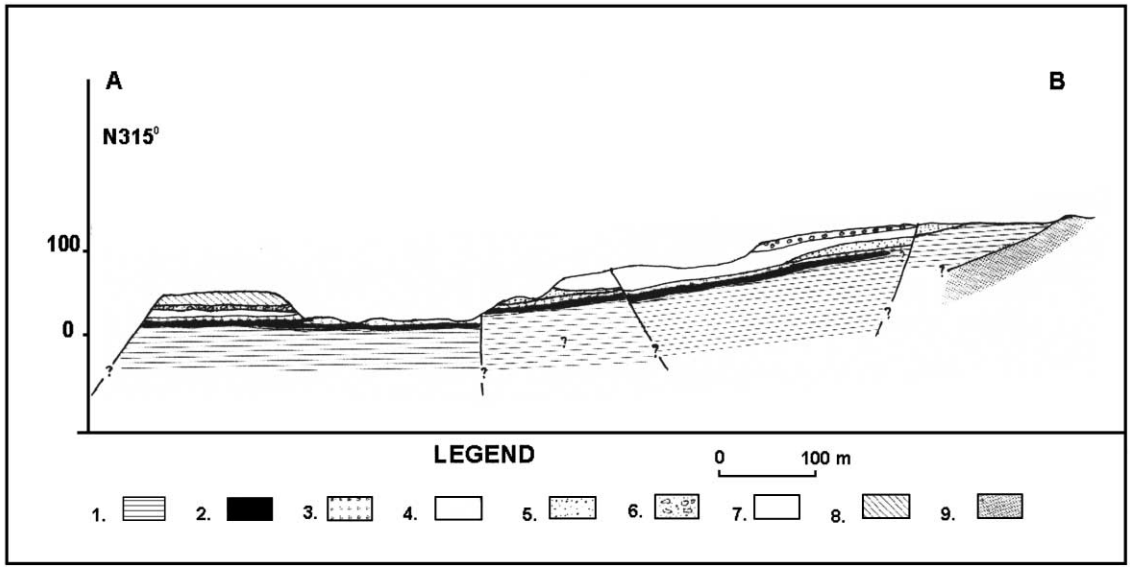

Fig. 5. Geological cross-section along the profile A–B (see Fig. 4 for location). (1) Underlying volcaniclastic sandstone; (2) manganese oxide beds; (3) green horizon (glauconitic); (4) white horizon (K-feldspar and oligoclase); (5) white horizon with arsenosiderite; (6) conglomerates; (7) overlying volcaniclastic sandstone; (8) soil horizon; (9) dacites (taken from Liakopoulos, 1987).

Subsequently, the deposit was studied as part of a doctoral thesis at the University of Paris (Liakopoulos, 1987), but only limited information about this deposit was published in English (Liakopoulos and Boulegue, 1987; Liakopoulos et al., 1986; Pflumio et al., 1991, 1993). In addition, the Greek Institute of Geology and Mineral Exploration (I.G.M.E.) undertook an exploration programme involving the drilling of 13 holes with an average depth of 30 m through the deposit between 1988 and 1989 in order to evaluate the economic importance of this deposit (Galanopoulos and Koinakis, 1991). Wetzenstein (1975), Hauck (1984), Kelepertzis and Kyriakopoulos (1991), Boström and Galanopoulos (1994), Hein et al. (1999, 2000) and Plimer (2000) have also discussed the origin of this deposit and Kelepertsis and Chatzitheodoridis (1989) have mapped the dispersion halos of various elements around the deposit. Hodkinson et al. (1994) have reported the enrichment of Mn, Cu, Zn and Pb in sediments just off the coast of the northern part of the central Milos embayment adjacent to Cape Vani and Karageorgis et al. (1998) presented data on the bathymetry, mineralogy and sediment geochemistry of Milos bay.

In summary, the Vani manganese deposit is an extremely well-preserved fossil stratabound hydrothermal deposit formed within an essentially undeformed and unmetamorphosed volcaniclastic sandstone. However, because the deposit is no longer of economic interest, it has not received the sort of attention that might have been expected on the basis of its unique characteristics. In this paper, we present a synthesis and critical discussion of the results of Liakopoulos (1987) for the first time in English in order to gain a better understanding of its nature and mode of origin. The following sections are based mainly on a translation of this work except where otherwise stated.

2.2. Mineralogy

Microscopic examination showed that the manganese-oxide minerals in the Vani manganese deposit form a cement in which fragments of volcaniclastic material occur. Two generations of manganese-oxide minerals were identified. The first generation consists of pyrolusite and ramsdellite; the second of oxides of the isostructural series cryptome-

lane–hollandite–coronadite plus hydrohetaerolite. The principal characteristics of these minerals have been described by Frenzel (1980), Roy (1981) and Post (1992). Post (1999) has recently reported that pyrolsite and ramsdellite may form in low-temperature hydrothermal deposits and the hollandite minerals may occur as prismatic crystals in hydrothermal veins.

2.2.1. First generation of manganese oxides

It is difficult to distinguish pyrolusite and ramsdellite under the microscope. They have very similar optical properties. Both are yellowish grey although pyrolusite is yellower than ramsdellite. What facilitates the differentiation is the system of cleavage and cracking, which is characteristic of ramsdellite (Fig. 7a, b). X-ray diffraction provides a better way to distinguish the two minerals because their symmetry is different. Pyrolusite is present either in a cryptocrystalline form or occurs in isolated zones within the ramsdellite. The dissemination of the pyrolusite in ramsdellite is thought to reflect the fact that it forms last as the more stable phase (Post, 1999).

2.2.2. Second generation of manganese oxides

If the discrimination between pyrolusite and ramsdellite under the microsope is difficult, that between the three minerals in the isomorphous series, cryptomelane–hollandite–coronadite is almost impossible. The similarity of the physical properties of these oxides is a consequence of the same crystal structure. The distinction based on X-ray diffraction studies is also not easy. The three oxides have the same symmetry and produce practically the same diffraction patterns. The intensity and position of the peaks vary only slightly and the minerals cannot be identified unambiguously based on these parameters alone. The only way to discriminate these minerals is by chemical analysis. This was achieved by means of the electron microprobe, in particular, by analyzing for K, Ba and Pb.

Hydrohaeterolite is easy to recognize under the optical microscope. It appears in close association with hollandite and occurs in irregular zones which are darker than those of hollandite (Fig. 7c).

Two generations of manganese oxides can be recognized under the optical microscope. The second generation of oxides polishes very easily and shows more reflecting zones which are whitish grey for the isomorphous series (cryptomelane–hollandite–coronadite; Fig. 7d) and brownish grey for hydrohetaerolite (Fig. 7c). The second generation of oxides occurs in the form of microcrystalline aggregates or with a rhythmic structure (e.g. coronadite; Fig. 7e) or in exsolution (hydrohaeterolite in hollandite; Fig. 7c). A problem may arise with hollandite, which sometimes forms needle-like crystals reminiscent of certain types of pyrolusite.

The oxides of the second generation replace the oxides of the first generation (Fig. 7b). In some cases, hydrothermal fluids have penetrated into the porous volcaniclastic sandstone to form lustrous manganese-oxide deposits with black metallic sheen on which botryoids of manganese oxides 2–15 mm in diameter have formed. The formation of lustrous manganese oxides with black metallic sheen is characteristic of submarine hydrothermal manganese deposits (Eckhardt et al., 1997; Glasby et al., 1997; Usui and Glasby, 1998). The oxides of the second generation, hollandite and coronadite, are seen to have developed on the outer parts of the botryoids, whereas the inner parts of the botryoids consist of the oxides of the first generation, notably ramsdellite, which are traversed by veins of hollandite or coronadite.

2.3. The replacement of the centre of feldspars by manganese oxides

We have already noted the presence of silicates in the manganese oxides. In polished sections under the optical microscope, these are seen to be K-feldspar (adularia) in which the central part of the crystal has been replaced by manganese oxides (Figs. 7f, 8B–F).

Based on numerous examinations under the microscope, it was shown that the oxide occupying the central part of the feldspar is always cryptomelane, hollandite (Fig. 7b–d) or coronadite (Fig. 8E, f; i.e. the oxides of the second generation). Our observations indicate that the initial introduction of the manganese oxides occurred during the sericitization of plagioclase. We believe that sericitization began at the periphery of the plagioclase crystal and migrated towards the centre along cleavage planes (Fig. 8A). The second phase of mineralization resulted in the introduction of additional K^+ ions which trans-

formed the sericite to K-feldspar and displaced the sericitized zone towards the centre of the crystal. Manganese then infiltrated the central part of the feldspar and replaced it.

2.4. Composition of the Mn oxides

The chemical compositions of the individual manganese-oxide phases or mineral pairs in the Vani deposit were determined by electron microprobe analysis (Tables 1 and 2). It was assumed that manganese exists entirely in the form of Mn^{4+} except for hydrohaeterolite where the manganese is mostly in the form of Mn^{3+} (Frenzel, 1980). The amount of Mn^{2+} determined by the oxalate method makes up 5% of the total manganese in cryptomelane and 10% in hollandite–coronadite. The problems associated with the separation of the three oxides mean that a precise determination of the amount of Mn^{2+} in each of these minerals was not possible.

Determination of the water content posed another problem. The adsorption of water by each mineral is facilitated by the very fine grain size of the manganese minerals as well as by the tunnel structures of cryptomelane, hollandite and coronadite. The water contents of pyrolusite and ramsdellite are both in the range 1–2%. For the isomorphous oxides, it is 4.3% for cryptomelane, in the range 0.0–7.2% for hollandite and 2% for coronadite.

2.4.1. Mn / Fe ratio

The Vani manganese oxides display a wide variability in their Mn/Fe ratios; ca. 130 for the first generation of manganese oxides (pyrolusite and ramsdellite), ca. 160 for cryptomelane–hollandite, ca. 500 for hollandite–coronadite, ca. 30 for hydrohetaerolite. These extremely high ratios reflect the well-known fractionation of manganese and iron during hydrothermal transport and mineralization (Glasby, 2000). Similar high Mn/Fe ratios have been observed in submarine hydrothermal manganese deposits from convergent plate margins at Kaikata Seamount on the Izu-Bonin Arc (Usui and Glasby, 1998) and Palinuro Seamount on the Aeolian Arc (Eckhardt et al., 1997). These high Mn/Fe ratios can be contrasted with the extremely low Mn/Fe ratios of other submarine hydrothermal oxyhydroxide deposits from the Aegean Arc as at Santorini (Boström et al., 1990a,b; Cronan et al., 2000) and Nisyros (Varnavas and Cronan, 1991; Rahders et al., 1999).

2.4.2. Co–Ni–Cu

The two generations of manganese oxides are characterized by very low concentrations of Co, Ni and Cu which, for the most part, do not exceed the detection limit of the electron microprobe (ca. 1000 ppm). This reflects the low contents of these elements in the hydrothermal fluids.

2.4.3. Second generation of manganese oxides

The structure of the oxides of the isomorphous series (cryptomelane–hollandite–coronadite) is based on an assemblage of octahedra (MnO_6), which link up in double chains along the *c*-axis to produce a three dimensional network. This structure has a pseudo-tetragonal structure containing large cavities (tunnels). These tunnels are filled with water molecules as well as the ions K^+, Ba^{2+} and Pb^{2+}, which are incorporated in cryptomelane, hollandite and coronadite, respectively.

2.4.3.1. Hollandite–coranadite. The minerals hollandite–coronadite display an excellent negative correlation between Ba and Pb ($r = -0.99$; Liakopoulos, 1987, pp. 52, Fig. 6). The divalent ions of these elements have similar ionic radii (1.34 Å for Ba and 1.20 Å for Pb) and substitute for each other. However, pure hollandite (17% BaO and 0% K_2O and PbO) and pure coronadite (30% PbO and 0% BaO and K_2O) account for only a small part of the mineralization at Cape Vani. Rather, the minerals present are dominantly intermediates in the isomorphous series hollandite–coronadite. The proportion of manganese oxides in the octahedral sites of hollandite–coronadite is inversely proportional to the sum of the oxides $K_2O + BaO + PbO$, which occupy vacant sites in the tunnels sites in these minerals (Liakopoulos, 1987, pp. 53, Fig. 7).

The hollandites–coronadites are also enriched in Zn with concentrations of up to 1.8% ZnO. They also contain up to 1.0% As_2O_3 (based on three analyses) (Table 1). The high concentration of As in the coronadite together with the previously noted presence of arseniosiderite close to the mineralized

Table 1
Electron microprobe analysis of selected elements in manganese oxide mineral pairs from the Vani manganese deposit
All analyses in percent.

	MnO_2	Fe_2O_3	K_2O	BaO	PbO	Al_2O_3	SiO_2	MgO	CoO	NiO	CuO	ZnO	Na_2O	CaO	As_2O_3	Total
1	69.2	n.d.	0.07	1.05	23.9	0.05	0.15	n.d.	0.04	n.d.	0.12	0.71	0.13	0.13	n.a	95.6
2	65.6	n.d.	0.06	0.1	30	n.a.	0.25	n.d.	0.05	n.d.	0.03	0.7	0.09	0.13	n.a	97
3	73.9	n.d.	0.61	5.77	13.2	0.05	0.26	0.03	n.d.	0.03	0.31	0.91	0.08	0.23	n.a	95.4
4	70.2	0.04	0.17	1.63	23.2	0.06	0.24	0.04	n.d.	n.d.	0.24	0.62	0.08	0.1	n.a	96.6
5	71.4	0.02	0.31	2.2	22.8	0.1	0.2	n.d.	n.d.	0.03	n.d.	0.3	n.d.	0.06	n.a	97.4
6	73.8	0.02	0.37	3.38	20.2	0.08	0.07	n.d.	n.d.	n.d.	0.21	0.21	n.d.	0.01	n.a	98.4
7	70.2	0.08	0.27	1.87	24.3	0.06	0.07	n.d.	n.d.	n.d.	n.d.	0.22	n.d.	n.d.	n.a	97
8	73.5	n.d.	0.39	2.59	20.8	0.06	0.05	n.d.	n.d.	n.d.	0.75	n.d.	n.d.	n.d.	n.a	98.1
9	72.2	n.d.	0.32	3.12	20.4	0.07	0.04	0.01	n.d.	n.d.	n.d.	0.11	0.01	n.d.	n.a	96.3
10	74.6	n.d.	0.69	4.13	19.1	0.07	0.06	0.03	0.04	n.d.	n.d.	0.28	0.11	n.d.	n.a	99.1
11	74.6	n.d.	0.78	11.9	2.96	0.18	0.16	0.21	n.d.	n.d.	n.d.	1.2	0.28	0.22	n.a	92.5
12	71.9	n.d.	0.55	6.04	13.9	0.16	0.05	0.18	n.d.	n.d.	0.73	1.79	0.27	0.24	n.a	95.8
13	72.5	0.8	0.23	2.21	21.8	0.03	0.28	n.d.	n.d.	n.d.	n.d.	0.99	n.d.	n.d.	n.a	98.8
14	70.8	0.58	0.13	0.88	26.3	0.07	0.31	0.03	n.d.	n.d.	0.15	1.16	n.d.	n.d.	n.a	100
15	82.2	n.d.	0.42	14.1	0.82	0.37	0.11	n.d.	0.23	0.05	1.54	0.71	n.d.	n.d.	n.a	101
16	71.1	0.03	0.62	7.27	11.4	0.19	0.15	0.16	n.d.	0.13	0.39	1.47	0.09	0.2	n.a	93.2
17	72.1	0.04	0.52	6.36	13.4	0.22	0.23	0.16	0.14	0.14	0.7	1.41	0.12	0.26	n.a	95.9
18	72.7	0.12	0.61	7.6	10.7	0.06	0.18	0.22	n.d.	0.07	0.44	0.63	0.22	0.13	n.a	93.7
19	70.6	n.d.	0.54	6.55	13	0.22	0.14	0.18	n.d.	n.d.	0.41	0.83	0.17	0.15	n.a	92.8
20	71.4	0.12	0.29	1.63	24	0.01	0.2	n.d.	n.d.	n.d.	0.13	0.28	0.07		n.a	98.2
21	71	0.06	0.17	0.87	25.2	0.06	0.14	n.d.	n.d.	n.d.	0.43	0.78	0.07	0.05	n.a	98.8
22	71.2	0.14	0.31	2.33	21.9	0.11	0.15	0.08	n.d.	n.d.	n.d.	0.84	0.19	0.1	n.a	97.4
23	71.6	n.d.	0.48	4.29	17.6	0.18	0.09	0.08	n.d.	0.01	n.d.	0.62	0.14	0.21	n.a	95.3
24	72.7	0.11	0.34	1.9	24.1	0.09	0.07	0.07	0.05	n.d.	0.01	1.02	0.03	0.17	n.a	101
25	70.2	0.13	0.23	1.95	23	0.04	0.07	0.02	n.d.	n.d.	0.39	0.62	0.02	0.13	n.a	96.8
26	69	n.d.	0.29	2.23	22.9	0.13	0.15	0.11	n.d.	0.06	0.29	0.71	0.05	0.2	n.a	94.1
27	71.8	0.05	0.2	2.04	21.9	0.19	0.15	0.08	n.d.	n.d.	0.14	0.88	0.13	0.08	n.a	97.7
28	70.3	0.18	0.14	0.78	24.6	0.01	0.23	0.11	0.1	n.d.	0.35	0.47	0.11	0.05	n.a	97.5
29	81	n.d.	0.75	14.8	1.48	0.33	0.01	0.07	n.d.	n.d.	0.31	0.65	0.1	0.09	n.a	99.4
30	72.3	0.13	0.79	4.05	16.8	0.11	0.34	0.08	0.34	n.d.	0.36	0.2	0.06	0.19	n.a	95.5
31	69.1	n.d.	n.d.	1.35	26.3	0.13	0.18	0.01	n.d.	n.d.	n.d.	0.16	0.05	0.15	n.a	97.4
32	71.4	0.15	0.25	2.63	20.8	0.07	0.26	0.08	n.d.	n.d.	0.12	0.41	0.12	0.06	n.a	96.4
33	68.3	0.04	0.08	1	26.2	0.01	0.35	0.01	n.d.	n.d.	0.17	0.47	n.d.	0.08	n.a	96.9
34	76.7	0.14	0.04	17.4	n.d.	0.5	0.12	0.07	n.d.	n.d.	n.d.	0.38	n.d.	n.d.	n.a	95.6
35	76.9	0.14	n.d.	16.9	n.d.	0.39	0.12	0.05	n.d.	n.d.	n.d.	0.2	n.d.	n.d.	n.a	94.7
36	72.2	n.d.	0.23	2.21	21.7	0.03	0.24	0.08	0.17	n.d.	0.33	1.24	n.d.	n.d.	n.a	98.1
37	73.5	0.08	0.17	1.45	21.9	0.05	0.4	0.02	0.13	n.d.	0.2	0.64	n.d.	n.d.	n.a	97.8
38	72.2	1.39	0.36	1.85	22.2	0.12	0.28	0.04	n.d.	0.12	0.4	0.67	n.d.	n.d.	n.a	99.6
39	72.2	n.d.	0.22	2.28	20.9	0.01	0.24	n.d.	n.d.	n.d.	n.d.	0.56	n.d.	n.d.	n.a	96.6
40	74.1	n.d.	0.25	2.76	18.4	0.08	0.1	0.06	n.d.	n.d.	n.d.	0.44	n.d.	n.d.	n.a	96.3
41	70.4	0.17	0.37	3.97	17.2	0.02	0.04	0.08	n.d.	n.d.	n.d.	n.d.	n.d.	n.d.	n.a	92.2
42	74.6	0.11	0.4	4.15	15.9	0.03	0.25	0.08	n.d.	n.d.	n.d.	n.d.	n.d.	n.d.	n.d	95.6
43	75.8	0.02	0.54	4.35	15.2	0.11	n.d.	n.d.	n.d.	0.05	n.d.	0.82	n.d.	n.d.	n.d	97.5
44	77.3	0.07	0.17	14	0.4	0.3	0.17	0.23	n.d.	0.11	0.12	0.18	n.d.	n.d.	n.d	93.1
45	79.9	n.d.	0.13	14.5	n.d.	0.12	0.21	0.18	0.02	n.d.	n.d.	n.d.	n.d.	n.d.	n.d	95
46	66	1.8	1.38	2.27	17.8	1.43	5.51	0.21	n.d.	0.08	0.16	0.86	n.d.	n.d.	n.d	97.5
47	73.9	0.33	0.35	2.45	21.2	0.12	0.26	0.04	n.d.	n.d.	n.d.	0.97	n.d.	n.d.	n.d	99.7
48	75.1	n.d.	0.28	2.34	19.6	0.02	0.26	n.d.	n.d.	0.08	n.d.	0.62	n.d.	n.d.	n.d	98.3
49	76.6	0.14	0.65	6.4	11.7	0.04	0.18	0.06	n.d.	n.d.	0.44	1.34	n.d.	n.d.	n.d	97.6
50	73.4	0.13	0.27	2.7	19.6	0.02	0.33	0.1	n.d.	n.d.	0.22	0.82	n.d.	n.d.	n.d	97.5
51	63.9	n.d.	n.d.	n.d.	27.9	n.a.	0.38	n.d.	n.d.	0.23	0.14	0.83	n.d.	0.17	1.9	95.5
52	65.9	0.78	n.d.	0.56	24.3	n.a.	0.21	n.d.	n.d.	n.d.	n.d.	0.54	n.d.	0.2	1.03	93.6

Table 1 (*continued*)

	MnO_2	Fe_2O_3	K_2O	BaO	PbO	Al_2O_3	SiO_2	MgO	CoO	NiO	CuO	ZnO	Na_2O	CaO	As_2O_3	Total
53	67.3	n.d.	n.d.	2.01	21.2	n.a.	0.21	n.d.	n.d.	0.03	n.d.	0.5	n.d.	0.29	0.9	92.5
54	72.3	n.d.	0.18	0.59	24.6	0.14	0.6	0.07	0.03	n.d.	n.d.	0.69	n.d.	n.d.	n.d	99.2
55	69.1	n.d.	0.15	0.98	26	0.01	0.32	0.04	n.d.	n.d.	n.d.	1.55	n.d.	n.d.	n.d	98.2
56	70.5	n.d.	0.12	n.d.	25.2	n.a.	0.36	0.02	n.d.	n.d.	0.04	0.36	n.d.	n.d.	n.d	97
57	71.4	n.d.	0.09	0.18	25.9	n.a.	0.29	n.d.	n.d.	n.d.	n.d.	0.22	n.d.	n.d.	n.d	98.5
58	74.9	n.d.	0.24	3.49	19.3	0.03	0.14	n.d.	n.d.	n.d.	0.09	0.58	n.d.	n.d.	n.d	98.7
59	79	n.d.	0.25	14.4	0.16	0.16	0.47	0.6	0.2	0.04	n.d.	n.d.	n.d.	0.21	n.d	95.4
60	83.8	0.02	0.36	4.43	4.8	0.43	0.12	0.12	n.d.	n.d.	0.08	1.49	n.d.	n.d.	n.d	95.6
61	85.56	n.d.	3.9	5.85	0.75	0.37	0.04	0.02	n.d.	n.d.	0.19	0.37	n.d.	0.12	n.a	97.2
62	82.9	n.d.	4.11	7.75	0.09	0.32	0.11	n.d.	n.d.	n.d.	0.17	0.33	n.d.	0.18	n.a	96
63	87.1	0.12	3.94	5.08	0.57	0.24	0.04	0.04	n.d.	0.13	0.23	0.67	n.d.	0.08	n.a	98.2
64	84.1	n.d.	4.42	5.81	1.18	0.25	n.d.	0.09	n.d.	n.d.	0.13	0.72	n.d.	0.08	n.a	96.8
65	85.4	n.d.	4.54	4.25	0.68	0.28	0.04	0.03	n.d.	n.d.	1.02	0.81	n.d.	0.11	n.a	97.1
66	81.2	0.34	4.38	7.62	0.12	0.47	n.d.	0.02	n.d.	n.d.	0.25	0.76	n.d.	0.07	n.a	95.6
67	80.27	0.27	3.33	9.49	0.29	0.31	n.d.	0.03	n.d.	1.57	0.01	0.42	n.d.	0.13	n.a	96.1
68	79.8	0.3	3.87	7.99	0.65	0.3	0.06	0.11	n.d.	n.d.	0.17	n.d.	n.d.	0.13	n.a	93.4
69	82.07	0.26	4.77	5.15	0.67	0.24	0.1	0.02	n.d.	n.d.	n.d.	0.94	n.d.	0.13	n.a	94.5
70	83.59	0.34	1.1	13.79	0.35	0.44	0.02	n.d.	n.d.	n.d.	0.14	n.d.	n.d.	0.12	n.a	99.9
71	83.6	0.3	3.72	3.94	n.d.	0.34	0.4	0.63	n.d.	n.d.	0.06	0.72	0.9	1.3	n.a	95.9
72	85	0.18	1.96	3.84	n.d.	0.42	0.47	0.52	n.d.	n.d.	0.08	n.d.	0.9	1.04	n.a	94.4
73	85.6	0.77	1.54	3.01	n.d.	0.44	0.36	0.81	n.d.	n.d.	n.d.	2.2	1	1.05	n.a	96.8
74	90.1	0.71	1.62	2.7	n.d.	0.33	0.36	0.74	n.d.	n.d.	0.13	0.41	1	0.89	n.a	98.9
75	81.9	0.21	5.07	11.4	n.d.	0.15	0.12	n.d.	n.d.	n.d.	0.23	0.32	0.3	0.14	n.a	99.8
76	82.23	2.19	6.13	3.49	n.d.	0.72	2.76	0.65	n.d.	0.05	n.d.	1.28	0.5	1.36	n.a	101
77	85.5	2.17	1.68	1.98	n.d.	0.94	3.31	0.84	n.d.	n.d.	0.3	0.17	0.8	0.91	n.a	98.6
78	77.42	0.17	0.95	13.18	n.d.	0.24	0.13	0.12	n.d.	n.d.	n.d.	1.16	0.3	0.3	n.a	94

n.d. = Not detected; n.a. = Not analyzed.
Samples 1–60: Coronadite–Hollandite.
Samples 61 to 78: Cryptomelane–Hollandite.

zone indicates that these two minerals were probably formed from the same hydrothermal fluid.

2.4.3.2. Cryptomelane–hollandite. In the case of the cryptomelane–hollandite, there is a negative correlation between K and Ba (Liakopoulos, 1987, pp. 55, Fig. 8). The proportion of manganese oxides is also inversely proportional to the sum of the oxides K_2O + BaO + PbO. The cryptomelane–hollandite is also enriched in Zn with concentrations of ZnO of up to 1.3% and Cu with concentrations of up to 1.0% CuO (Table 1).

2.4.3.3. Hydrohaeterolite. Hydrohaeterolite is isomorphous with hausmannite and displays a tetragonal structure. In the Cape Vani manganese oxides, hydrohaeterolite appears to be in exsolution in hollandite. Electron microprobe analysis shows that the hydrohaeterolite contains up to 1.5% BaO and up to 0.62% K_2O (Table 2). Pb also occurs sporadically in hydrohaeterolite. As is present in hydrohaeterolite only in low concentrations. Zn occurs in hydrohaeterolite in concentrations of up to 33.6% ZnO. ZnO shows a negative correlation with K_2O + BaO + PbO in hollandite–hydrohaeterolite; however, the mixing between these minerals is not continuous.

2.5. Accessory minerals

2.5.1. Barite

Field and laboratory investigations demonstrated that there are two generations of barite at Cape Vani. The first generation of barite is disseminated in the volcaniclastic sandstone. Some of this barite has been cemented and replaced by manganese oxides of the second generation. Microcrystalline K-feldspar (adularia) is often seen to have formed around barite crystals associated with the manganese-oxide layers

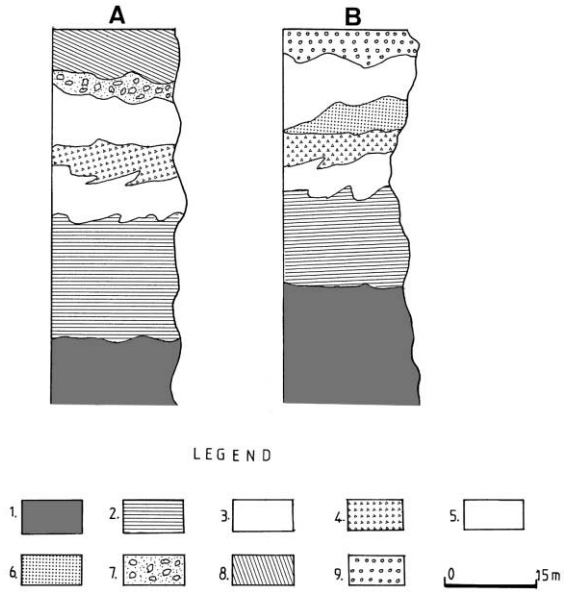

Fig. 6. Schematic representation of the stratigraphy of manganese mineralization at Cape Vani. Profile A is from the western sector of Cape Vani and B from the western sector. (1) Dacites; (2) underlying volcaniclastic sandstone; (3) manganese oxide beds; (4) green horizon (glauconitic); (5) white horizon (K-feldspar and oligoclase); (6) white horizon with arsenosiderite; (7) conglomerates; (8) overlying volcaniclastic sandstone; (9) soil horizon (taken from Liakopoulos, 1987, p. 43).

(Fig. 7d). In some cases, iron oxyhydroxides have also formed concentrically around the barite crystals. The second generation of barite appears in the form of veins 5–15 cm thick, which cut the manganese ore and the dacites. The preferred directions of the veins are about N330° and N30°. Apart from barite and quartz, which are the principal constituents of the veins, sulphides (sphalerite and galena) are also observed.

2.5.2. Arseniosiderite

Arseniosiderite occurs in the red layer within the white horizon as described previously. The occurrence of different forms of this mineral was demonstrated by means of electron microprobe analysis. Under the microscope, the arseniosiderite is yellow or reddish brown and occurs either as an assemblage of fibrous crystals radiating around a centre or as isolated crystals, both types of which are cemented within a ferruginous matrix. The average composition of this mineral based on the electron microprobe analysis of 14 spots was 30.0% Fe_2O_3, 31.9% As_2O_5, 12.8% CaO, 4.5% SiO_2, 1.5% MnO_2 and 0.15% Al_2O_3.

2.6. Vein mineralization in the Mn oxides at Kondaros

The most important indications of sulphides are located at Kondaros, which is situated south of Mt. Katsimoutis (Fig. 4). These consist of vein mineralization in the manganese oxides that develop at the NE extremity of a major fault. This fault is oriented almost N30° and extends to the SW as far as Triades. The fault cuts intensively fractured and altered dacites. Secondary minerals found there include kaolinite, sericite and adularia. The principal vein mineralization is about 1 m thick and is oriented almost N30°. The dacites are traversed by a number of veins which display no preferred orientation and vary in thickness between 5 and 10 cm. Microscopic observation shows that this mineralization consists of sulphides (sphalerite, galena, chalcopyrite and pyrite), carbonates (calcite, manganocalcite), barite and quartz. Quartz and carbonates are the most important constituents of the veins (> 90%). Sphalerite is the dominant sulphide mineral. The sulphides occur either in small veins or disseminated in a carbonate and siliceous matrix.

2.7. Hydrothermal alteration associated with the deposition of the Mn oxides

2.7.1. Zones of hydrothermal alteration

More than 100 samples were taken in the vicinity of Vani manganese deposit as well as from the volcaniclastic sandstone and volcanic rocks surrounding this area in order to study the influence of hydrothermal alteration on the geology of the area. As a result of this study, the following secondary minerals were identified by X-ray diffraction, optical microscopy and electron microprobe analysis: K-feldspar, K-mica, chlorite, kaolinite, montmorillonite and silica. Fig. 9 shows the distribution of the products of hydrothermal alteration, which was based not only on the presence or absence of a particular mineral phase, but also on the nature of the dominant

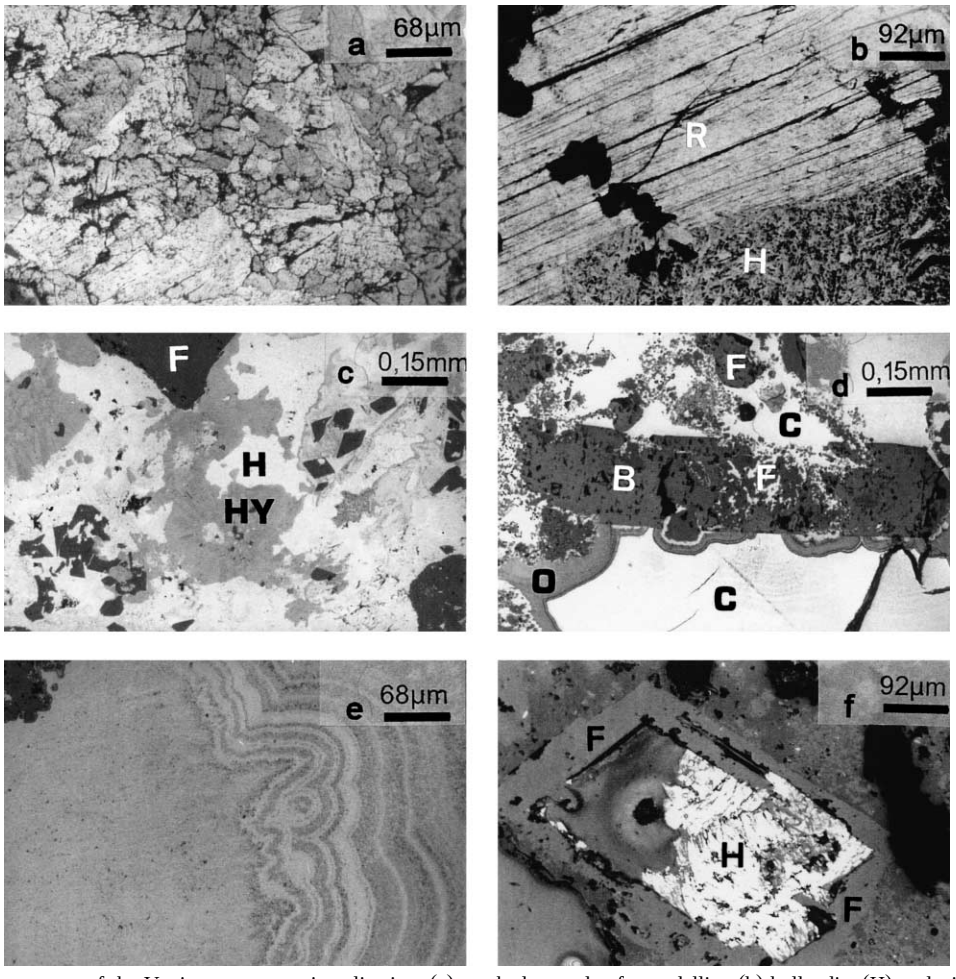

Fig. 7. Different aspects of the Vani manganese mineralization: (a) cracked crystals of ramsdellite; (b) hollandite (H) replacing ramsdellite (R); (c) exsolutions forms of hydrohetaerolite (Hy), hollandite (H) and K-Feldspar (F); (d) dissolution of barite (B) by coronadite (C), presence of ferric oxides (O) and microcrystals of K-feldspar (F); (e) coronadite displaying a rhythmic structure; (f) replacement of K-feldspar (F) by hollandite (H).

mineral phase. Four distinct mineralogical zones were identified dominated by K-feldspar, montmorillonite, kaolinite and sericite, and kaolinite and cristoballite, respectively. Minor amounts of oligoclase, K-feldspar and montmorillonite were observed in the overlying volcaniclastic sandstone of the mineralized zone.

2.7.1.1. K-feldspar zone. The Vani manganese deposit is closely associated with the K-feldspar zone. The mineral constituents of the volcaniclastic sandstone and underlying dacites were transformed mainly into K-feldspar with lesser amounts of K-mica. Chlorite, leucoxene and silica were present as secondary minerals. The compositions of the K-feldspars are presented in Table 3.

2.7.1.2. Intermediate zone of montmorillonite. The montmorillonite zone comprises montmorillonite, K-feldspar and sericite. The montmorillonite was identified by X-ray diffraction on oriented samples. Under the microscope, the montmorillonite was seen to occur as spheroidal, microcrystalline aggregates with a weak yellow colour which developed at the expense of the plagioclase and the rock matrix.

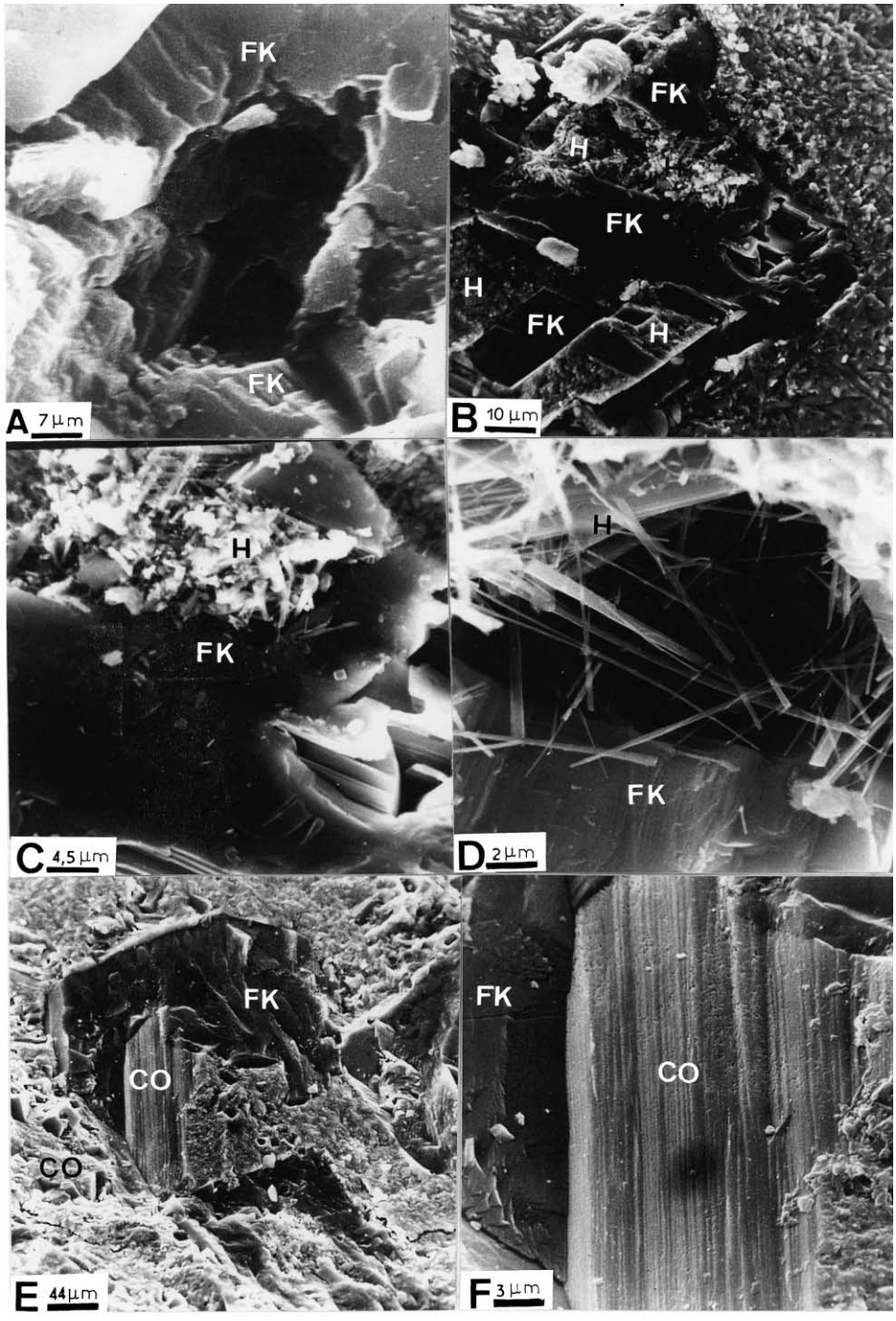

Fig. 8. SEM photographs showing different aspects of K-feldspar replacement by the second generation of manganese oxides: (A) existence of cavities in the K-feldspar crystals (FK); (B–D) hollandite (H) replacing K-feldspar (FK); (E–F) coronadite (CO) replacing K-feldspar (FK).

Table 2
Electron microprobe analysis of selected elements in manganese oxide mineral pairs from the Vani manganese deposit
All analyses in percent.

	MnO_2	Fe_2O_3	K_2O	BaO	PbO	ZnO	As_2O_3	SrO	Au	F	Total
1	54.76	2.04	0.46	0.31	n.d.	32.89	n.d.	n.d.	n.d.	n.d.	90.45
2	56.07	2.6	0.38	n.d.	n.d.	31.9	0.05	n.d.	n.d.	0.08	91.08
3	56.15	2.69	0.35	n.d.	n.d.	31.61	n.d.	n.d.	n.d.	0.03	90.84
4	55.96	1.77	0.4	n.d.	n.d.	31.5	0.04	n.d.	0.07	0.25	89.98
5	57.64	2.5	0.18	n.d.	n.d.	31.9	0.05	0.16	n.d.	0.33	92.77
6	55.46	2.44	0.19	0.06	n.d.	32.9	n.d.	n.d.	0.04	n.d.	91.1
7	57.82	2.37	0.17	0.07	0.06	32.14	n.d.	n.d.	0.01	0.03	92.67
8	56.07	0.55	0.21	n.d.	n.d.	33.65	0.2	n.d.	n.d.	n.d.	90.5
9	57.32	2.11	0.22	n.d.	n.d.	31.4	0.07	n.d.	0.09	n.d.	91.2
10	56.16	1.46	0.13	0.02	n.d.	32.4	n.d.	n.d.	n.d.	0.06	90.2
11	55.37	1.18	0.55	1.51	0.15	27.14	n.d.	n.d.	n.d.	0.17	86.07
12	57.12	0.7	0.33	1.06	n.d.	30.6	0.26	0.16	n.d.	0.58	90.8
13	54.89	1.19	0.62	1.18	0.06	26.24	0.1	n.d.	n.d.	0.28	84.56
14	55.37	0.87	0.5	1.04	0.12	28.68	0.08	n.d.	n.d.	0.2	86.86
15	53.97	1.06	0.56	0.98	n.d.	26.9	n.d.	n.d.	0.06	n.d.	83.53
16	54.47	0.84	0.52	1.38	n.d.	27.65	0.06	0.02	n.d.	0.03	84.97
17	55.07	0.84	0.44	1.54	n.d.	24.72	0.04	n.d.	n.d.	n.d.	82.65
18	57.09	0.12	0	0.07	n.d.	32.67	n.d.	n.d.	n.d.	0.2	90.15
19	57.06	0.04	0	n.d.	0.01	32.68	0.11	0.07	0.02	n.d.	89.98
20	53.36	0.71	0.19	0.07	n.d.	32.95	n.d.	0.02	0.19	n.d.	87.48
21	54.47	2.6	0.2	0.13	n.d.	33.57	n.d.	n.d.	n.d.	0.16	91.13
22	52.38	2.74	0.3	0.06	0.03	32.47	0.06	n.d.	0.13	n.d.	88.16
23	54.91	2	0.22	0.09	n.d.	32.06	n.d.	n.d.	0.04	n.d.	89.64
24	53.95	2.34	0.23	0.15	0.24	32.09	0.04	n.d.	0.09	0.27	89.11
25	80.19	0.08	0.29	12.87	0.05	3.27	0.11	0.26	n.d.	n.d.	97.12
26	78.33	0.04	0.15	13.17	0.01	3.37	0.45	0.11	0.12	0.45	96.21
27	80.15	0.08	0.15	13.43	n.d.	2.68	0.16	n.d.	0.01	0.16	96.83
28	74.38	0.35	0.65	7.42	0.29	4.88	n.d.	0.2	n.d.	0.34	88.51
29	71.95	0.53	0.6	7.76	0.42	5.5	0.24	0.33	n.d.	n.d.	87.32
30	70.04	1.36	1.04	7.73	0.58	4.35	0.2	0.05	0.09	n.d.	85.44
31	68.63	0.98	0.81	7.56	2.75	2.83	0.32	0.09	0.07	0.13	84.16
32	71.11	2.78	0.57	8.34	0.26	4.91	n.d.	0.33	n.d.	n.d.	88.3
33	66.25	1.56	0.53	5.54	12.5	2.14	0.25	n.d.	0.03	0.05	88.84
34	73.71	0.11	0.62	7.92	0.4	4.32	n.d.	0.26	n.d.	n.d.	87.34

n.d. = Not detected.
Samples 1–34: Coronadite–Hydrohaeterolite.

2.7.1.3. Kaolinite zone. The kaolinite zone occurs in the outer parts of the Vani basin where kaolinite along with K-feldspar and K-mica have developed at the expense of plagioclase. In certain places, alteration is more advanced resulting in the complete argillization of the rock with the mineralogical assemblage dominated by kaolinite and cristobalite. However, there is no clear evidence that the kaolinization process was related to the manganese mineralization at Vani. Pflumio et al. (1991) have shown that the kaolinized lavas have the same Sr isotopic ratios as the unaltered dacites. This suggests that argillization was not related to the hydrothermal alteration processes at Vani and may post-date the manganese mineralization.

2.7.1.4. Dacites. The dacites occur as domes or lava flows. Samples of unaltered dacites were taken on the northern slope of Mt. Katsimoutis (Fig. 3). Microscopically, these dacites consist of a porphyric, microlitic and sometimes fluidal structures and are characterized by a microcrystalline matrix consisting

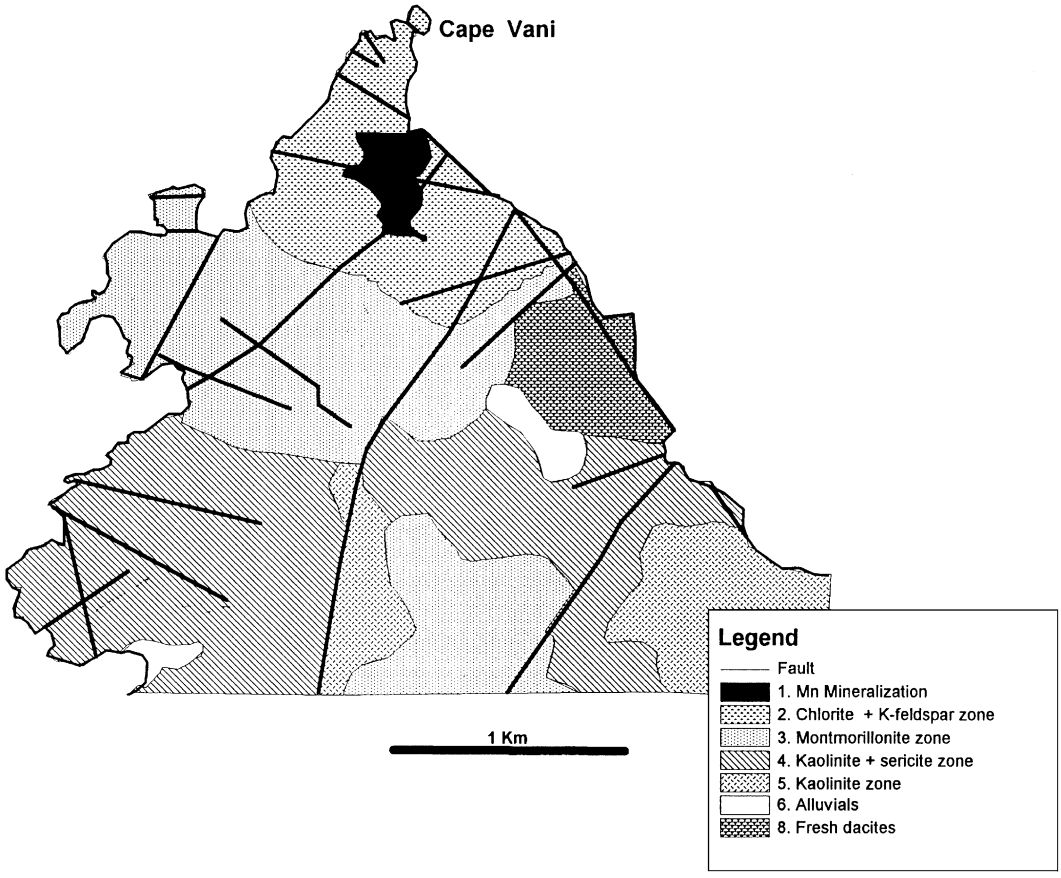

Fig. 9. Schematic map showing the distribution of the products of hydrothermal alteration around the Vani manganese deposit.

of rods of plagioclase, quartz and volcanic glass. They are composed principally of andesine-labrador plagioclase, pyroxenes, amphiboles, biotites, quartz and titanomagnetites. The altered dacites occur within the Vani basin and show metasomatic phenomena with neoformation of adularia, sericite and chlorite. They are characterized by an enrichment of K_2O and depletion of CaO, MgO and Na_2O compared to the unaltered dacites. The compositions of the unaltered and altered dacites are presented in Table 4.

3. Mineralization at Triades—Galana

Galana, the ancient mining area of Triades, is situated about 4 km south of the Vani manganese deposit. There is some evidence for limited mining of this deposit in Roman times (Plimer, 2000). The mining company Siphnos-Eubée exploited the deposit from 1884 until the beginning of the 20th century, first for Pb–Zn and shortly afterwards for Ag. Mining was mainly open cast although mining also took place at depth in the Galana mine by means of a system of galleries which, in some cases, descended 75 m below sea level (Liakopoulos, 1987). Reserves of the mine were estimated to be 10 million tonnes on a dry weight basis with an mean concentration of Ag of 500 ppm. The principal Ag minerals present were argentite (Ag_2S) and pyrargyrite (Ag_3SbS_3). Two types of barite could be distinguished, an almost pure barite and one very rich in silica. Both types of barite are argentiferous with Ag

Table 3
Electron microprobe analysis of selected elements in K-feldspar minerals from the Vani area
All analyses in percent.

	K_2O	Al_2O_3	SiO_2	Na_2O	CaO	BaO	MnO	PbO	FeO	MgO	CuO	ZnO	Total
1	17.96	17.97	64.38	n.d.	n.d.	n.d.	n.d.	n.d.	0.01	n.d.	n.d.	n.d.	100.32
2	17.37	18.11	64.33	n.d.	n.d.	n.d.	n.d.	n.d.	n.d.	0.03	0.08	0.17	100.09
3	18.02	18.15	63.95	n.d.	n.d.	n.d.	n.d.	n.d.	0.02	n.d.	0.05	0.18	100.37
4	18.24	18.41	63.72	n.d.	n.d.	n.d.	n.d.	n.d.	n.d.	n.d.	0.04	n.d.	100.41
5	16.39	18.1	64.51	n.d.	n.d.	n.d.	n.d.	n.d.	0.01	0.02	0.56	n.d.	99.59
6	17.89	18.17	63.53	n.d.	n.d.	n.d.	n.d.	n.d.	n.d.	n.d.	n.d.	n.d.	99.59
7	15.14	19.37	63.98	n.d.	n.d.	0.47	n.d.	n.d.	0.05	0.2	0.1	0.1	99.31
8	17.76	17.94	63.28	n.d.	n.d.	0.12	n.d.	0.24	n.d.	n.d.	0.11	n.d.	99.45
9	17.86	17.73	61.93	n.d.	n.d.	n.d.	n.d.	0.25	n.d.	n.d.	n.d.	0.31	98.08
10	18.11	17.63	64.98	0.07	n.d.	0.02	0.28	0.12	n.d.	n.d.	0.02	0.01	101.24
11	16.95	17.64	65.49	n.d.	n.d.	0.02	0.19	n.d.	n.d.	n.d.	n.d.	0.22	100.51
12	17.67	17.85	65.7	n.d.	n.d.	n.d.	n.d.	n.d.	0.31	0.06	n.d.	n.d.	101.59
13	17.47	17.99	65.01	n.d.	n.d.	n.d.	0.36	0.05	n.d.	0.03	n.d.	n.d.	100.91
14	17.2	18.02	64.42	n.d.	n.d.	n.d.	0.11	0.01	n.d.	n.d.	n.d.	n.d.	99.76
15	16.93	17.72	64.77	n.d.	n.d.	n.d.	0.48	n.d.	n.d.	0.04	n.d.	n.d.	99.94
16	17.1	17.73	64.5	n.d.	n.d.	n.d.	0.58	n.d.	n.d.	n.d.	n.d.	0.23	100.14
17	17.54	17.58	65.89	n.d.	n.d.	n.d.	0.51	0.11	n.d.	n.d.	n.d.	n.d.	101.63
18	16.71	17.57	64.91	n.d.	n.d.	0.14	0.46	n.d.	0.08	n.d.	0.08	n.d.	99.95
19	16.6	17.62	65.14	n.d.	n.d.	n.d.	0.57	n.d.	n.d.	n.d.	n.d.	n.d.	99.93
20	17.24	18.2	64.08	n.d.	n.d.	0.21	0.99	0.06	0.07	0.04	n.d.	n.d.	100.89
21	17.81	17.6	65.12	n.d.	n.d.	n.d.	0.05	n.d.	n.d.	n.d.	n.d.	0.15	100.73
22	18.03	17.75	65.77	n.d.	n.d.	n.d.	0.31	n.d.	0.28	0.02	n.d.	n.d.	102.16
23	16.8	17.97	64.34	n.d.	n.d.	0.68	0.07	0.08	n.d.	n.d.	n.d.	n.d.	99.94
24	17.06	17.76	65.04	n.d.	n.d.	n.d.	n.d.	n.d.	0.07	n.d.	n.d.	n.d.	99.93
25	17.65	17.96	63.4	n.d.	n.d.	0.17	0.48	n.d.	0.04	n.d.	n.d.	n.d.	99.7
26	15.4	18	68.95	0.38	0.09	0.03	n.d.	n.d.	0.05	n.d.	n.d.	n.d.	102.9
27	16.82	18.72	65.38	0.33	n.d.	0.48	0.06	n.d.	0.08	n.d.	n.d.	n.d.	101.87
28	15.63	18.16	66.28	0.57	0.11	n.d.	0.08	n.d.	n.d.	n.d.	0.07	0.02	100.92
29	17.11	18.28	65.75	0.04	n.d.	n.d.	n.d.	0.19	0.02	n.d.	n.d.	n.d.	101.39
30	16.16	18.62	64.25	0.21	n.d.	0.89	0.24	0.11	n.d.	0.02	n.d.	0.01	100.51
31	16.31	18.66	66.65	0.13	n.d.	0.07	0.23	n.d.	n.d.	0.04	n.d.	n.d.	102.09
32	13.42	19.28	64.32	1.31	0.4	0.64	0.94	0.18	0.1	n.d.	0.11	n.d.	100.7
33	12.6	19.09	67.1	1.27	0.26	0.18	n.d.	0.11	0.62	n.d.	0.16	0.19	101.58
34	13.73	18.68	66.58	0.79	0.16	0.01	n.d.	0.04	0.12	n.d.	n.d.	0.01	100.12
35	12.98	18.59	66.41	1.48	0.18	0.06	0.07	0.16	0.12	0.02	n.d.	n.d.	100.07
36	16.18	17.12	63.72	0.12	n.d.	0.01	n.d.	n.d.	0.02	n.d.	n.d.	0.02	97.19
37	16.71	17.73	65.44	0.13	n.d.	n.d.	n.d.	n.d.	0.3	n.d.	n.d.	n.d.	100.31
38	17.22	18.6	65.55	0.09	n.d.	n.d.	n.d.	n.d.	0.25	n.d.	n.d.	0.01	101.72
39	15.08	19.47	58.76	0.04	0.03	3.53	n.d.	n.d.	0.08	n.d.	n.d.	0.08	97.07
40	15.24	19.27	65.82	0.07	0.05	n.d.	0.05	n.d.	0.02	n.d.	n.d.	n.d.	100.52
41	13.14	25.41	59.95	0.05	0.02	1.41	0.43	n.d.	n.d.	n.d.	n.d.	n.d.	100.41
42	17.6	19.15	64.9	0.08	0.01	0.48	0.01	n.d.	0.24	0.14	0.18	n.d.	102.79
43	17.68	18.6	63.06	0.07	n.d.	0.14	0.09	0.16	n.d.	n.d.	0.08	n.d.	99.88
44	18.07	17.73	64.28	0.05	n.d.	n.d.	n.d.	n.d.	n.d.	n.d.	n.d.	0.08	100.21
45	16.51	18.79	61.78	0.1	n.d.	1.69	0.09	n.d.	0.14	n.d.	n.d.	0.02	99.12
46	16.97	19.16	63.14	0.007	n.d.	1.94	n.d.	n.d.	n.d.	n.d.	n.d.	n.d.	101.22
47	11.15	19.63	64.03	1.87	0.2	n.d.	0.07	0.23	n.d.	0.02	n.d.	n.d.	97.2
48	14.72	18.92	65.53	1.63	0.18	0.59	n.d.	0.05	1.09	0.27	n.d.	n.d.	102.98
49	14.78	19.92	61.73	0.2	n.d.	2.91	n.d.	0.22	0.52	n.d.	n.d.	n.d.	100.28
50	14.92	18.06	65.35	0.12	n.d.	0.02	n.d.	n.d.	n.d.	0.06	n.d.	n.d.	98.53
51	16.76	18.19	66.69	0.11	n.d.	n.d.	n.d.	n.d.	0.26	n.d.	n.d.	0.14	102.15

(continued on next page)

Table 3 (*continued*)

	K_2O	Al_2O_3	SiO_2	Na_2O	CaO	BaO	MnO	PbO	FeO	MgO	CuO	ZnO	Total
52	15.64	19.08	66.22	0.36	n.d.	n.d.	n.d.	n.d.	0.19	0.16	n.d.	0.3	101.95
53	14.63	18.36	63.72	0.38	n.d.	n.d.	n.d.	n.d.	1.8	1.24	n.d.	0.02	100.15

Number of specific ions on the basis of eight oxygens

	K	Al	Si	Na	Ca	Ba	Total	Ab%	An%	Or%
1	0.191	0.259	2.143				2.59	0.00	0.00	100.00
2	0.184	0.533	2.141				2.86	0.00	0.00	100.00
3	0.191	0.534	2.128				2.85	0.00	0.00	100.00
4	0.194	0.542	2.121				2.86	0.00	0.00	100.00
5	0.174	0.533	2.147				2.85	0.00	0.00	100.00
6	0.19	0.535	2.114				2.84	0.00	0.00	100.00
7	0.161	0.57	2.129			0.003	2.86	0.00	0.00	100.00
8	0.189	0.528	2.106			0.0008	2.82	0.00	0.00	100.00
9	0.19	0.522	2.06				2.77	0.00	0.00	100.00
10	0.192	0.519	2.163	0.01		0.0001	2.88	4.95	0.00	95.05
11	0.18	0.519	2.18			0.0001	2.88	0.00	0.00	100.00
12	0.188	0.525	2.187				2.90	0.00	0.00	100.00
13	0.185	0.529	2.164				2.88	0.00	0.00	100.00
14	0.183	0.53	2.144				2.86	0.00	0.00	100.00
15	0.18	0.521	2.156				2.86	0.00	0.00	100.00
16	0.182	0.522	2.147				2.85	0.00	0.00	100.00
17	0.186	0.517	2.193				2.90	0.00	0.00	100.00
18	0.177	0.517	2.16			0.0009	2.85	0.00	0.00	100.00
19	0.176	0.519	2.168				2.86	0.00	0.00	100.00
20	0.183	0.536	2.133			0.001	2.85	0.00	0.00	100.00
21	0.189	0.518	2.167				2.87	0.00	0.00	100.00
22	0.191	0.522	2.189				2.90	0.00	0.00	100.00
23	0.178	0.529	2.141			0.004	2.85	0.00	0.00	100.00
24	0.181	0.523	2.165				2.87	0.00	0.00	100.00
25	0.187	0.529	2.11			0.001	2.83	0.00	0.00	100.00
26	0.902	0.975	3.031	0.034	0.004	0.0005	4.95	3.62	0.43	95.96
27	0.98	1.007	2.986	0.029		0.009	5.01	2.87	0.00	97.13
28	0.909	0.976	3.022	0.051	0.006		4.96	5.28	0.62	94.10
29	0.999	0.986	3.008	0.003			5.00	0.30	0.00	99.70
30	0.956	1.018	2.979	0.019		0.016	4.99	1.95	0.00	98.05
31	0.94	0.994	3.01	0.011		0.001	4.96	1.16	0.00	98.84
32	0.784	1.041	2.945	0.116	0.02	0.011	4.92	12.61	2.17	85.22
33	0.724	1.013	3.02	0.111	0.013	0.003	4.88	13.09	1.53	85.38
34	0.796	1.001	3.026	0.07	0.008	0.0001	4.90	8.01	0.92	91.08
35	0.748	0.997	3.021	0.131	0.009	0.001	4.91	14.75	1.01	84.23
36	0.981	0.958	3.027	0.011	0.009	0.002	4.99	1.10	0.90	98.00
37	0.985	0.965	3.022	0.012			4.98	1.20	0.00	98.80
38	0.989	0.997	2.98	0.008			4.97	0.80	0.00	99.20
39	0.944	1.126	2.883	0.004	0.002	0.068	5.03	0.42	0.21	99.37
40	0.994	1.027	2.977	0.006	0.002		5.01	0.60	0.20	99.20
41	0.767	1.331	2.745	0.004	0.001	0.025	4.87	0.52	0.13	99.35
42	1.025	1.03	2.963	0.007	0.001	0.009	5.04	0.68	0.10	99.23
43	1.059	1.029	2.959	0.006	0.0003	0.26	5.31	0.56	0.03	99.41
44	1.075	0.974	2.997	0.004			5.05	0.37	0.00	99.63
45	1.002	1.054	2.939	0.009		0.031	5.04	0.89	0.00	99.11
46	1.008	1.051	2.939	0.006		0.036	5.04	0.59	0.00	99.41
47	0.657	1.068	2.956	0.167	0.01		4.86	20.02	1.20	78.78
48	0.852	1.011	2.973	0.144	0.009		4.99	14.33	0.90	84.78

Table 3 (*continued*)

	Number of specific ions on the basis of eight oxygens									
	K	Al	Si	Na	Ca	Ba	Total	Ab%	An%	Or%
49	0.89	1.108	2.915	0.018		0.054	4.99	1.98	0.00	98.02
50	0.883	0.988	3.033	0.011			4.92	1.23	0.00	98.77
51	0.97	0.97	3.02	0.01			4.97	1.02	0.00	98.98
52	0.9	1.01	2.99	0.03			4.93	3.23	0.00	96.77
53	0.86	1	2.94	0.03			4.83	3.37	0.00	96.63

n.d. = Not detected.
Samples 1–25: K-feldspar secondary minerals from the Vani maganese area.
Samples 26–32: K-feldspar minerals from the volcanoclastic sandstone area.
Samples 33–53: K-feldspar minerals from the altered dacite area.

contents of up to 1000 g tonnes^{-1}. This deposit may be considered to be an example of epithermal gold mineralization (Spartali, 1994).

Locally, the geological formations are intensively silicified and form irregular large blocks coloured red by iron oxides. Barite and sulphide mineralization is intimately associated with the silicified zones. At the surface, mineralization consists of barite + quartz + sulphides disseminated in the siliceous matrix; however, at depth, it takes the form of sulphide veins and lens-shaped bodies of barite. The mineralization like the alteration of the rocks is linked with the direction of the faults at N30° and E–W.

Two main phases of mineralization have been identified. The first resulted in the formation of sphalerite, galena, chalcopyrite, grey copper (tennandite tetrahydrite), pyrite, cerussite and barite and the second in the formation of covellite, azurite, malachite and anglesite. This phase of mineralization is thought to represent the remineralization of sul-

Table 4
Chemical analysis of selected elements in unaltered and altered dacites from the Vani area
All analyses in percent.

	SiO_2	Al_2O_3	Fe_2O_3	FeO	TiO_2	CaO	MgO	Na_2O	K_2O	H_2O	Total
Unaltered dacites											
Vd-84-2	62.13	16.8	4.15	1.9	0.67	6.64	2.65	3.34	1.63	0.1	100.01
TR-84-7	65.2	17.01	1.87	2.96	0.61	4.45	2.81	3.18	1.87	0.07	100.03
TRN2	64.92	16.86	1.47	2.98	0.61	5.27	2.33	3.57	1.88	0.1	99.99
F-84-5	61.42	16.66	2.27	3.51	0.67	6.74	3.57	3.21	1.82	0.13	100
F-85-2	61.74	17.29	1.68	3.95	0.59	6.42	3.07	3.07	1.88	0.12	99.81
Vd-2	61.34	16.57	4.1	1.87	0.66	6.56	2.62	3.3	1.61	0.44	99.07
Average	62.79	16.87	2.59	2.86	0.64	6.01	2.84	3.28	1.78	0.16	99.82
Altered dacites											
Vd-84-1	65.75	15.99	2.27	2.7	0.54	0.58	2.52	0.73	8.76	0.1	99.94
Vd-85-1	67.96	16.66	2.6	0.37	0.55	0.06	0.88	0.64	10.3	0.1	100.12
Vd-84-3	66.51	17.05	2.08	0.44	0.58	0.58	0.67	0.4	11.44	0.11	99.86
Vd-84-4	62.84	16.92	3.94	0.74	0.45	2.02	1.66	1.28	10.07	0.13	100.05
Vd-84-5	63.07	17.15	3.38	0.89	0.45	1.73	1.99	1.4	9.83	0.11	100
Vd-85-12	67.01	18.14	3.61	0.59	0.64	0.7	0.84	0.22	8.26	0.11	100.12
Vd-85-20	66.39	17.1	4.06	0.44	0.54	3.45	0.08	2.68	5.26	0.1	100.1
Vd-85-22	59.69	19.53	3.71	1.19	0.8	0.06	1.75	0.15	12.79	0.2	99.87
Average	64.90	17.32	3.21	0.92	0.57	1.15	1.30	0.94	9.59	0.12	100.01

Unaltered Dacites: Samples Vd-84-2 and Vd-2 from Vani area (Katsimoutis). Samples Tr-84-7 and TRN2 from North Triades (south of the Vani area). Samples F/84/5 and F-85-2 from Plaka (for comparison).
Altered Dacites: All samples from the Vani area.

phides and barite deposited at depth. Data on the mineralogy and composition of this deposit have been reported by Vavelidis and Melfos (1998). Christanis and Seymour (1995) have pointed to the importance of boiling of the hydrothermal fluid from the deep geothermal reservoir at temperatures of ca. 310 °C and depths of ca. 1000 m in the deposition of the sulphides at Triades.

4. Hydrothermal origin of the Vani Mn deposit

Milos Island is part of the Aegean Arc which lies at the boundary of the African and Aegean plates. This situation has resulted in typical calc-alkaline volcanism and a much elevated geothermal gradient.

The immense hydrothermal activity on Milos affected the volcanic formations and metamorphic and sedimentary basement. The evolution of the present geothermal field suggests that there has long been a convective hydrothermal system on the island and that this system developed in two main stages. The initial stage of submarine hydrothermal activity took place in the western part of the island in the vicinity of the Vani basin and resulted in the deposition of manganese oxides, barite and sulphides. The subsequent phase of subaerial hydrothermal activity took place mainly in the eastern part of the island and continues to this day. It resulted in the formation of clays (kaolinite, bentonite), sulphates (barite, alunite) and silica. Differences in mineralization can be related to the fact that the hydrothermal system in some places in the western sector of Milos was dominated by the liquid phase, whereas the hydrothermal system in the eastern sector of Milos is dominated mainly by the vapour phase.

Oxygen and hydrogen isotopic data of present-day geothermal fluids on Milos have shown that the fluid from the deep geothermal reservoir is derived from seawater and undergoes subsurface liquid-vapour phase separation (Liakopoulos, 1987; Liakopoulos and Boulegue, 1987; Pflumio et al., 1991, 1993). This has resulted in marked enrichments in Mn, Fe, Pb and Zn in samples of high-salinity geothermal fluids taken from the well-head and suggests that phase separation in the geothermal fluids may have been an important factor in the formation of metallogenic deposits on the island. Sr isotopic data determined for geothermal fluids, fresh lavas, basement greenschists and manganese oxides indicate that the Sr in the mineralizing fluids of both fossil and active hydrotheral systems was derived from the same source, namely the greenschist basement. By contrast, Pb isotopic data on the same samples suggest that Pb in the present-day mineralizing fluid is derived from both the basement and volcanics, but that an additional, more radiogenic source of Pb contributed to the isotopic composition of the fluids during the period of manganese mineralization (Pflumio et al., 1991, 1993).

In the western sector of Milos Island, volcanism began in the Upper Pliocene with the formation of dacitic domes and lavas. The end of the emplacement of the dacites was marked by the collapse of the magma chamber, which resulted in a huge pyroclastic episode and the deposition of a thick layer of pyroclastic material below sea level. The collapse of the magma chamber in combination with local tectonic events caused extensive fracturing of the host rock, which led to the infiltration of seawater to depth within the system. The heat supplied during cooling resulted in the reaction of the seawater with the dacite to form a hot, acidic solution enriched in various metals.

From the available evidence, we can envisage that the deposition of the manganese oxides in the Vani area took place in two principal phases. In the initial phase, the hydrothermal fluid deposited the first generation of manganese oxides, pyrolusite and ramsdellite, in the volcaniclastic sandstone of the Vani submarine basin. This phase was also characterized by the formation of barite disseminated in the sandstone and the possible deposition of sulphides at depth (cf. Glasby, 2000; Hein et al., 2000). In the later phase, the arrival of a second hydrothermal fluid in the Vani basin led to the deposition of the second generation of manganese oxides, cryptomelane–hollandite–coronadite plus hydrohaeterolite, barite and arseniosiderite. Mineralogical studies showed that the manganese oxides developed by replacement of the first generation of manganese oxides, which was accompanied by the dissolution of the barite. The existence of the second generation of oxides suggests that the fluid responsible for its formation must have been enriched in Ba, Pb, Zn and As. It is believed that this enrichment was

caused by the dissolution of sulphides deposited at depth during the initial phase of hydrothermalism (cf. Petersen et al., 2000).

Fig. 10 is a *P–T* diagram which shows the two possible processes which led to the deposition of the Cape Vani manganese oxides. The figures have been constructed based on the behaviour of the present-day geothermal system in Milos.

Fig. 10a illustrates the process occurring during the initial mineralizing phase. It is assumed that the hydrostatic pressure was sufficiently high that phase separation of the fluid did not occur in the deep geothermal reservoir. The rise of the fluid led to a progressive decrease in the pressure and temperature, which resulted in phase separation of the fluid in the lower sections of the mineralized zone with the

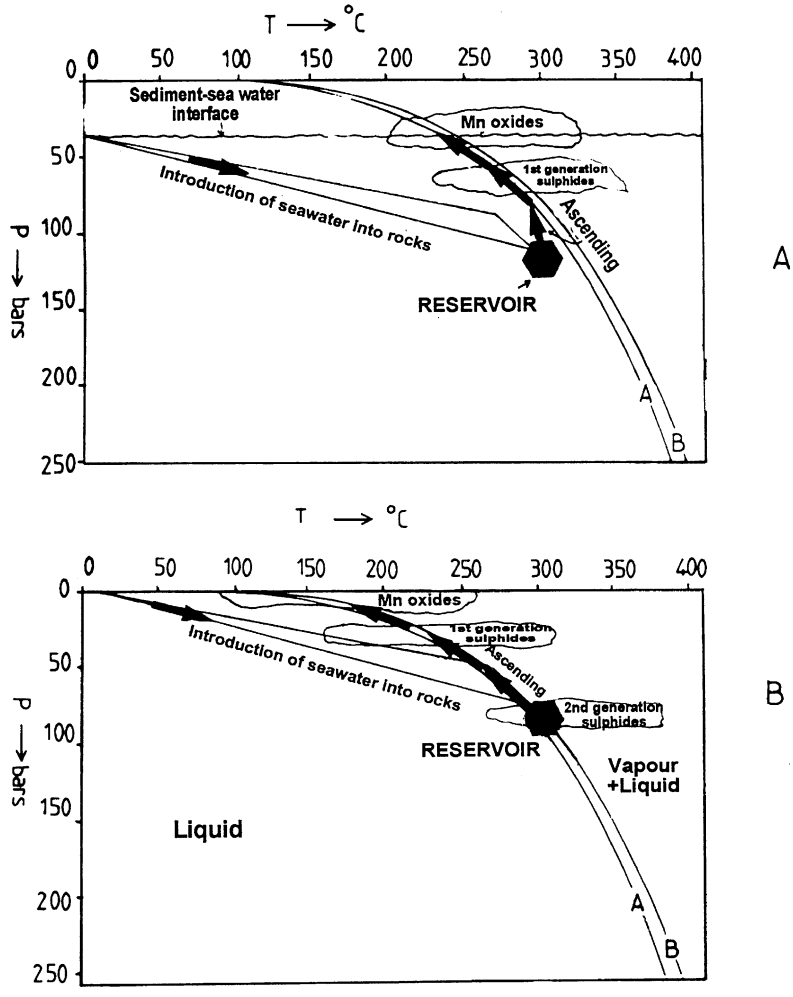

Fig. 10. Consists of two temperature–pressure diagrams indicating the two phase boundary for seawater containing 3.2% NaCl (taken from Bishoff and Rosenbauer, 1984) and for a brine containing 10% NaCl (taken from Hass, 1971). For comparison, the geothermal brine in the eastern sector of Milos has a chloride content of 1.6 mol l^{-1} (or 9.4% NaCl) (Liakopoulos, 1987). (A) Illustrates the processes occurring during the formation of the first generation of manganese oxides when the existing pressure did not permit boiling and phase separation to take place in the deep reservoir (taken from Liakopoulos, 1987). (B) Illustrates the processes occurring during the formation of the second generation of manganese oxides when boiling and phase separation occurred in the reservoir (taken from Liakopoulos, 1987).

consequent precipitation of the sulphides. The fluid subsequently impregated the volcaniclastic sandstone and mixed with cold, oxygenated seawater. This led to the deposition of the first generation of manganese oxides and of disseminated barite within the sandstone.

In the later phase, tectonic uplift of the basin permitted phase separation of the fluid to take place in the geothermal reservoir, possibly resulting in the precipitation of sulphides (Fig. 10b). On rising to the surface, the hydrothermal vapour mixed with seawater and reacted with the dacite leading to the kaolinitization and silicification of the host rock. In addition, the hydrothermal fluid further altered the dacite, reacted with the sulphides and sulphates formed during the initial metallogenic phase and became enriched in Ba, Pb and Zn. As is very mobile under acidic conditions and was probably extracted from arseniferous minerals.

The second generation of manganese oxides resulted from the interaction of this latter fluid with the first generation of manganese oxides. The manganese was derived not only from the hydrothermal solution, but also from the dissolution of the first generation manganese oxides (pyrolusite and ramsdellite) and was deposited in the form of cryptomelane–hollandite–coronadite plus hydrohetaerolite. The second generation of manganese oxides was, therefore, formed by the replacement of the first generation of oxides.

5. Discussion

The preceeding sections are based mainly on a translation of the work of Liakopoulos (1987). We would now like to make some additional comments on the origin of the Vani manganese deposit.

Most interestingly, the studies reported here confirm the unique features of this deposit. In particular, the Vani manganese deposit is quite different in mineralogy and composition from most known terrestrial and submarine hydrothermal manganese deposits, reflecting its particular mode of origin (e.g. Crespo and Lunar, 1997; Miura and Hariya, 1997; Rey et al., 1997). Of the terrestrial hydrothermal manganese deposits described by Roy (1968, 1981, 1992, 1997), only the hydrothermal vein deposits rich in manganese plus the Inimi deposit from Morocco described by Force and Cannon (1988) show any similarity to Vani manganese deposit in terms of mineralogy and composition.

Kelepertzis and Kyriakopoulos (1991) have suggested that the Lucifer manganese deposit from Baja California Sur, Mexico (Freiberg, 1983) and the San Francisco manganese deposit from Jalisco, Mexico (Zantop, 1978, 1981) show many similarities to the Vani manganese deposit. However, the Lucifer deposit is a stratiform manganese deposit in which the manganese is interstratified with tuffaceous conglomerates and tuffaceous limestones. In the San Francisco deposit, the manganese and iron oxides are stratigraphically conformable with the tuffaceous host rocks and were thought to have deposited from hydrothermal solutions in a lacustrine basin. By contrast, the Vani manganese deposit is a hydrothermal stratabound deposit in which the deposition of the manganese oxides is controlled by fissure- and pore-filling.

Boström and Galanopoulos (1994) have also claimed similarity of the Vani manganese deposit with the Precambrian Långban deposit of Sweden based on the high contents of Mn, Fe and Ba in these deposits (cf. Boström et al., 1979; Holtsam and Langhof, 2000). However, the Långban deposit contains recoverable amounts of iron and manganese oxides within a single gallery in the mine, whereas the Vani manganese deposit is characterized by very low Fe contents. This difference means that these two deposits cannot be considered exact analogues. Boström and Galanopoulos (1994) have also suggested that Vani and Långban deposits are both volcanic-exhalative deposits in which much of the Mn, Fe and Ba were mobilized from marine sediments in a subduction zone of an island arc. This hypothesis is not in accordance with the strictly hydrothermal origin presented here.

However, the most similar deposits to the Vani deposit appear to be the epithermal vein deposits of the southwestern United States and elsewhere described by Hewett (1964, 1971). These deposits consist mainly of psilomelane, cryptomelane, hollandite, coronadite and, less commonly, pyrolusite and ramsdellite and have been described by Roy (1968) as hypogene vein deposits. They are characterized by the persistent veins of barite and fluorite and, in

many cases, occur in close proximity to explored deposits of these minerals. There is generally a zoned arrangement of the veins of oxides and other minerals within the deposit. Arseniosiderite is also an accessory mineral in many of these deposits. The host rocks are mainly layered volcanic rocks of Tertiary age with persistent alteration of plagioclase in the host rock to K-feldspar (adularia). These deposits also tend to be associated with epithermal gold and epithermal base-metal sulphide deposits. However, these deposits are fault-controlled and occur in the form of veins which may be up to 1.5 m thick, extend horizontally up to 500 m and can be traced to depths of up to 150 m. Significantly, both Hewett (1964) and Roy (1968) concluded that these vein deposits formed in the upper reaches of the epithermal system as a result of mixing of ascending hydrothermal fluids with descending meteoric water enriched in oxygen. Indeed, Roy (1968) attributed the formation of these higher oxides of manganese to the high concentrations of oxygen and falling temperatures. Although these deposits are not exact analogues of the Vani manganese deposit, they do show sufficient similarity to suggest a similar mode of origin.

By contrast, the Franklin (New Jersey) deposit is a highly metamorphosed Precambrian deposit. Although it is suggested that the hydrothermal manganese may have originally precipitated as psilomelane, cryptomelane and hollandite, the degree of metamorphism is such that it is not realistic to compare this deposit with the Vani deposit (Frondel and Baum, 1974).

Submarine hydrothermal manganese deposits, on the other hand, tend to be characterized by high Mn/Fe ratios and low contents of Ni, Cu, Zn, Co, Pb and detrital silicate minerals with 10 Å manganate as the principal manganese-oxide mineral (Eckhardt et al., 1997; Glasby et al., 1997; Usui and Glasby, 1998; Glasby, 2000). They are, therefore, quite different in mineralogy and composition from the Vani deposit. The Vani manganese deposit is also much thicker than any known submarine hydrothermal manganese deposit. This reflects the fact that it was formed by the replacement of the volcaniclastic sandstone, which effectively trapped most of the hydrothermal manganese in its matrix. This contrasts to most modern submarine hydrothermal systems where the bulk of the manganese is discharged directly into sea water (Lavelle et al., 1992). The greater thickness of this deposit compared to known submarine hydrothermal manganese deposits indicates either a very much longer time scale of formation or a much faster growth rate than for submarine hydrothermal manganese deposits.

If we assume that the rate of formation of the Vani deposit is the same as that of submarine hydrothermal manganese deposits (in excess of 5–25 m 10^6 year^{-1}, Burgath and von Stackelberg, 1995) and that the deposit has a thickness of about 4 m, then we can calculate that this deposit would have formed over a period of 0.2–1.0 Ma. If, however, we assume that this deposit formed within $<$ 125,000 years (the age of the TAG hydrothermal Field, Scott, 1997), this would imply a growth rate for the deposit of $>$ 32 m 10^6 year^{-1}, which is considerably higher that that of modern submarine hydrothermal manganese deposits. However, high-temperature massive sulphide deposition at the TAG Field only started somewhat in excess 20,000 years ago (Petersen et al., 2000). If the Vani deposit formed on a similar time scale, this would imply a growth rate of about 200 m 10^6 year^{-1}, which is more than an order of magnitude faster than for submarine hydrothermal manganese deposits. In this regard, it is significant that Hein et al. (1990) have identified three types of stratabound hydrothermal manganese deposits from the Tonga–Lau region: a spreading axis type, a Tonga Ridge type and an insular type (cf. Hein et al., 1997). These stratabound deposits are characterized by high Mn/Fe ratios and growth rates in the range of tens of metres 10^6 year^{-1} compared to normal submarine hydrothermal manganese deposits which have growth rates in the range of metres 10^6 year^{-1}. These calculations suggest that the Vani manganese deposit may have formed even faster than the stratabound manganese deposits from the Tonga–Lau region.

The environmental setting of the Vani manganese deposit at its time of formation remains problematic. The discovery of marine fossils in the volcaniclastic sandstone of the Vani basin indicates that the sandstone was deposited in a submarine setting, but tells us nothing about the environment in which the hydrothermal manganese deposit was formed. Two factors may have influenced the environmental setting

of the Vani manganese deposit: sea level change and tectonic uplift. According to Fytikas et al. (1989), earthquakes on Milos have a tectonic rather than a volcanic origin.

Tectonic uplift in the Vani area has been estimated to have been about 250 m in the past 0.8 Ma (Papanikolaou et al., 1990). This corresponds to an uplift rate for the area of about 320 m 10^6 year^{-1} (or about 0.32 mm year^{-1}), which is significantly higher than the uplift/subsidence rates of about 0.2 mm year^{-1} previously reported for the Aegean region (Le Pichon and Angelier, 1981), but is consistent with their high levels of tectonic activity on Milos. Plimer (2000) has noted that an old cobble beach located 50 m up a cliff above the present cobble beach cuts the manganese-oxide layers in the western part of the Vani manganese deposit confirming the rapid uplift of the Vani deposit since its formation.

The Vani manganese deposit presently occurs between 35 m above sea level and an unknown depth below sea level. Assuming that the deposit formed within the volcaniclastic sandstone at a depth of somewhere between 50 and 250 m below sea level about 2 Ma, we can calculate an overall uplift rate for the deposit of about 25–125 m 10^6 year^{-1} (or about 0.02–0.12 mm year^{-1}). This is well within the known uplift rates in the Aegean. Although this calculation is subject to a large margin of error, it does demonstrate that the Vani manganese deposit could well have formed in a submarine setting.

Plimer (2000) has argued that the earth was an icehouse at the time of formation of the Vani manganese deposit. Although the sea level curves of Haq et al. (1987) do indeed indicate a drop in sea level of about 80 m in the period from 2.9 to 2.0 Ma, we have no age data to support this idea.

Based on our field observations, we believe that the volcaniclastic sandstone at Cape Vani was deposited in a submarine environment and subsequently compacted with the development of vertical joints (fissures) within its structure. Hydrothermal fluids were able to penetrate these fissures and migrated along the bedding plane of the sandstone. Hydrothermal manganese mineralization was, therefore, controlled by the distribution of these fissures and the porosity of the sandstone. Based on this model, the Vani manganese deposit is not a submarine hydrothermal manganese deposit in the strict sense of the term, but rather a stratabound hydrothermal deposit.

Faults are known to play a key role in hydrothermal mineralization (Glasby, 1998). Fytikas et al. (1989) have stressed the importance of faults on Milos Island in active fluid transport at shallow depths in the earth's crust and Dando et al. (2000) have established that modern submarine hydrothermal venting is located along fault lines and is most intense where faults intersect. Cape Vani lies proximal to the Vromolimni–Kondaro fault which marks the western boundary of Milos bay (Fig. 1). We believe that movement along this fault may have played a key role in triggering the hydrothermal activity which resulted in the formation of the Vani manganese deposit. At present, intense manganese deposition associated with the NNW–SSE-trending fault is presently taking place on the eastern side of Milos bay near Skinopi.

Although considered to be a hydrothermal manganese deposit, the Vani deposit is unusual in combining high Mn/Fe ratios with high contents of K, Ba, Pb and Zn. As already suggested, this is a consequence of a two-stage process of formation of the manganese-oxide minerals in which a second hydrothermal fluid enriched in Ba, Pb, Zn and As formed as a result of the dissolution of sulphide minerals by a saline hydrothermal fluid, which remineralized the original manganese-oxide assemblage to produce the characteristic cryptomelane–hollandite–coronadite plus hydrohetaerolite assemblage. It is this two-stage process of formation which, more than anything else, has contributed to the unique features of this deposit.

An important parameter is the temperature of deposition of the manganese oxides in the Vani deposit. According to Liakopoulos (1987), exhaustive studies have shown that the geothermal waters of the modern deep geothermal reservoir in the central-eastern part of Milos have a temperature of 318 °C at a depth of 1150–1200 m, a pH of 4.5–4.7 and are in thermodynamic equilibrium with K-mica (Liakopoulos, 1987; Liakopoulos et al., 1991). On the basis of oxygen isotopic analysis, Liakopoulos (1987) also calculated that the temperature of deposition of the calcite veins at Kontaros was 180 ± 35 °C and that their formation required the mixing of the

mineralizing fluid with seawater. Most significantly, however, Roy (1981, 1997) has reported that cryptomelane, hollandite and coronadite occur in the uppermost, low-temperature hydrothermal manganese veins of hypogene manganese deposits and in hot spring apron deposits (cf. Hewett, 1964). Although no temperature data are available for the formation of the Cape Vani manganese oxides, it would, therefore, appear probable that these deposits were formed as late-stage, low-temperature deposits. For comparison, submarine hydrothermal manganese deposits typically form in the range 5–25 °C (Burgath and von Stackelberg, 1995).

Despite these findings, several open questions remain regarding the origin of the Vani manganese deposit.

(i) In his thesis, Liakopoulos (1987) described the setting of the Vani manganese deposit as a submarine caldera. This description is based on the earlier conclusion of Hauck (1984) that certain types of mineralization on Milos, such as barite and sulphide formation, were the result of Kuroko-type ore deposition. However, there is no geological or geophysical evidence for caldera formation in the Vani region at present. We have, therefore, chosen to describe this area as the Vani volcano-sedimentary basin.

(ii) It is still not fully resolved whether the Vani manganese deposit is a submarine hydrothermal deposit or not. Hauck (1984) considered that manganese mineralization at Vani took place in a NW-oriented, slightly sloping marine basin, which had been filled by a 50-m-thick layer of material consisting mostly of coarse blocks of pumice, which also contained marine mussels encrusted in manganese oxides. Hauck (1984) also determined the sulphur isotopic ratio of barite from Vani and obtained a mean value of $\delta^{34}S$ of +21‰, which is similar to that of modern seawater (+20‰), indicating that seawater dominated the hydrothermal fluid from which the barite was formed. Hein et al. (2000) also concluded that the dominant mineralizing fluid was derived from seawater on the basis of REE contents and Sr and S isotopic ratios of the manganese deposit and associated barite.

(iii) According to Mendrinos (1988), the Milos geothermal field is characterized by the existence of two different flow systems separated by a caprock of low permeability. The deeper flow system consists of a high-salinity fluid which flows in from the sea, becomes further enriched in chloride through phase separation and steam loss, rises adiabatically and vents on the seafloor. The chloride content of this fluid is, on average, 45‰ compared to 21‰ for normal seawater. Submarine geothermal systems off Milos are all derived from this deep geothermal reservoir. This type of system could be the source of the geothermal fluids that formed the Vani manganese deposit.

The date of emplacement of the host volcaniclastic sandstones as well as the relative ages of the two generations of the Vani manganese deposit remain unknown. These questions are particularly important to understanding the mode of manganese mineralization. The tectonic setting and the extent of hydrothermal alteration of the host rocks at Cape Vani also remain poorly known.

(iv) In spite of these uncertainties, we consider that Vani manganese deposit most probably formed in a shallow, submarine setting in which a thick layer of pyroclastic material had been deposited and lithified to produce a porous volcaniclastic sandstone. Hydrothermal fluids enriched in Mn, Ba, Pb, Zn from leaching the schist basement and dacitic host rocks penetrated the sandstone horizons via fractures and fissures. The permeable nature of the sandstone facilitated the retention of the hydrothermal fluids in these layers. This permitted the fluids to cool slowly and deposit the manganese oxides almost quantitatively. Formation of the hydrothermal manganese deposit took place fairly rapidly over a period of several tens of thousands of years at most. Strong tectonic activity resulted in rapid uplift of the area which elevated the deposit above sea level.

6. Conclusions

From our study, a number of conclusions concerning the origin of the Vani manganese deposit have emerged.

(1) The Vani manganese deposit is a stratabound hydrothermal manganese deposit formed within porous volcaniclastic sandstone during the Upper Pleistocene. Deposition of the manganese oxides was controlled by the distribution of fissures within the sandstone and the porosity of the sandstone.

(2) The deposit was formed in a shallow marine environment. However, it differs significantly from normal submarine hydrothermal manganese deposits in both mineralogy and composition. It is also characterized by much higher growth rates than submarine hydrothermal manganese deposits as a result of the almost quantitative deposition of the manganese oxides within the matrix of the volcaniclastic sandstone.

(3) The deposit is believed to have formed in two main stages. The first generation of manganese oxides (pyrolusite and ramsdellite) is considered to be a late stage, low-temperature mineral deposit trapped in a porous medium. The second generation of manganese oxides (cryptomelane–hollandite–coronadite plus hydrohaeterolite) formed as a result of the alteration of the first generation of manganese oxides during a later phase of hydrothermal activity in which the hydrothermal fluids were enriched in K, Ba, Pb, Zn and As.

(4) The only close analogue of the Vani manganese deposit appears to be the epithermal vein deposits of the southwestern United States. These are similar in mineralogy and composition to the Vani deposit, but are epithermal vein deposits, whereas the Vani deposit is a stratabound hydrothermal deposit. They cannot, therefore, be considered exact analogues. The Vani manganese deposit, therefore, appears to be unique.

(5) Strong tectonic activity resulted in rapid uplift of the area which elevated the deposit above sea level. Movement along the Vromolimni–Kondaro fault may have played a key role in triggering the hydrothermal activity which resulted in the formation of the Vani manganese deposit.

Acknowledgements

A. Liakopoulos is grateful to the scientific and technical team of the laboratory of geochemistry and metalogenesis of the Université Pierre et Marie Curie for their scientific and technical support. He also wishes to thank Dr. E.A. Perseil from the Laboratory of Mineralogy of the Museum of Natural History (Paris) from her help in the determination of the manganese minerals and for scientific discussion. During his thesis, he was awarded a fellowship by the Hellenic State Foundation and the Bodossakis Foundation. G.P. Glasby was an EU Marie Curie senior fellow for the duration of this project in Athens. We would like to thank Prof. M. Fytikas, Dr. T. Kuhn, Prof. D. Papanikolaou, Prof. N. Skarpelis and an anonymous referee for their helpful comments.

References

Angelier, J., Cantagrel, J.M., Vilminot, J.C., 1977. Néotectonique cassante et volcanisme plioquaternaire dans l'arc égéen interne: l'île de Milos (Grèce). Bull. Soc. Géol. Fr. 7 (XIX), 119–124.

Anonymous, 199a. Greek treasure. Min. J. 332 (8513) Jan. 1/8, 1–2.

Anonymous, 199b. Milos encouragement. Min. J. 332 (8536) June 18, 457.

Argyropoulos, G., 1966. Montangeologische Beurteilung der Mn-Lagerstätte von Cap Vani, Milos. Unpubl. Diplom Arbeit (Univ. Leoben), 69 pp.

Bishoff, J.L., Rosenbauer, R.J., 1984. The critical point and two phase boundary of sea water, 200–500 °C. Earth Planet. Sci. Lett. 68, 172–180.

Boström, K., Galanopoulos, V., 1994. The origin of volcanic-exhalative deposits rich in Fe, Mn, and Ba: a comparison of the Vani and Långban deposits. Bull. Geol. Soc. Greece 30 (3), 225–239.

Boström, K., Rydell, H., Joensuu, O., 1979. Långban—an exhalative sedimentary deposit? Econ. Geol. 74, 1002–1011.

Boström, K., Hallberg, A., Åberg, A., Magmet de Saissy, H., 1990a. Metallogenesis at Santorini—a subduction-zone related process: I. Deposition of hydrothermal sediments. Thera and the Aegean World III, vol. 2. Thera Foundation, London, pp. 280–290.

Boström, K., Perissoratis, C., Galanopoulos, V., Papavassiliou, C., Boström, B., Ingri, J., Kalogeropoulos, S., 1990b. Geochemistry and structural control of hydrothermal sediments and new hot springs in the caldera of Santorini. Thera and the Aegean World III, vol. 2. Thera Foundation, London, pp. 325–336.

Burgath, K.-P., von Stackelberg, U., 1995. Sulfide-impregnated volcanics and ferromanganese incrustations from the southern Lau Basin (southwest Pacific). Mar. Georesourc. Geotechnol. 13, 263–308.

Christanis, K., Seymour, K.St., 1995. A study of scale formation: an analogue of meso- to epithermal ore formation in the volcano of Milos, Aegean Arc, Greece. Geothermics 24, 541–552.

Christidis, G.E., Scott, P.W., Marcopoulos, T., 1995. Origin of the bentonite deposits of Eastern Milos, Aegean, Greece: Geological, mineralogical and geochemical evidence. Clays Clay Miner. 43, 63–77.

Crespo, A., Lunar, R., 1997. Terrestrial hot-spring Co-rich Mn mineralization in the Pliocene–Quaternary Calatrava Region

(central Spain). In: Nicholson, K., Hein, J.R., Bühn, B., Dasgupta, S. (Eds.), Manganese Mineralization: Geochemistry and Mineralogy of Terrestrial and Marine Deposits. Geol. Soc. Spec. Publ., vol. 119, pp. 253–264.

Cronan, D.S., Varnavas, S.P., Hodkinson, R., 2000. Hydrothermal mineralizing processes and associated sedimentation in Santorini hydrothermal embayments. Mar. Georesourc. Geotechnol. 18, 77–118.

Dando, P.R., Stüben, D., Varnavas, S.P., 1999. Hydrothermalism in the Mediterranean Sea. Proc. Oceanogr. 44, 333–367.

Dando, P.R., Aliani, S., Arab, H., Bianchi, C.N., Brehmer, M., Cocito, S., Fowler, S.W., Gundersen, J., Hooper, L.E., Kölbl, R., Kuever, J., Linke, P., Makropoulos, K.C., Meloni, R., Miquel, J.-C., Morri, C., Müller, S., Robinson, C., Schlesner, H., Sievert, S., Stöhr, R., Stüben, D., Thomm, M., Varnavas, S.P., Ziebis, W., 2000. Hydrothermal studies in the Aegean Sea. Phys. Chem. Earth (B) 25, 1–8.

Delibasis, N.D., Drakopoulos, J.C., 1993. The Milos Island earthquake of March 20, 1992 and its tectonic significance. Pure Appl. Geophys. 141, 43–58.

Eckhardt, J.-D., Glasby, G.P., Puchelt, H., Berner, Z., 1997. Hydrothermal manganese crusts from Enareta and Palinuro Seamounts in the Tyrrhenian Sea. Mar. Georesourc. Geotechnol. 15, 175–208.

Force, E.R., Cannon, W.F., 1988. Depositional model for shallow-marine manganese deposits around black-shale basins. Econ. Geol. 83, 93–117.

Freiberg, D.A., 1983. Geological setting and origin of the Lucifer manganese deposit, Baja California Sur, Mexico. Econ. Geol. 78, 931–943.

Frenzel, G., 1980. The manganese oxide minerals. In: Varentsov, I.M., Grasselly, Gy. (Eds.), 1980. Geology and Geochemistry of Manganese, vol. I. Hungarian Academy of Sciences, Budapest, pp. 25–157.

Frondel, C., Baum, J.L., 1974. Structure and mineralogy of the Franklin zinc–iron-manganese deposit, New Jersey. Econ. Geol. 69, 157–180.

Fytikas, M., 1977. Geological and geothermal study of Milos Island. Inst. Geol. Min. Res. Geol. Geophys. Res. 18 (1), 228 pp. + 32 plates + 3 maps.

Fytikas, M., 1989. Updating of the geological and geothermal research on Milos Island. Geothermics 18, 485–496.

Fytikas, M., Marinelli, G., 1976. Geology and Geothermics of the Island of Milos (Greece). International Congress on Thermal Waters, Geothermal Energy and Volcanism of the Mediterranean Area. Institute of Geology and Mineral Exploration, Athens, pp. 1–58.

Fytikas, M., Markopoulos, Th., 1992. 6th Congress of the Geological Society of Greece Post-Congress Field Trip to Milos May 28–30, 1992 Guide Book, 34 pp.

Fytikas, M., Innocenti, F., Kolios, N., Manetti, P., Mazzuoli, R., Poli, G., Rita, F., Villari, L., 1986. Volcanology and petrology of volcanic products from the island of Milos and neighbouring islets. J. Volcanol. Geotherm. Res. 28, 297–317.

Fytikas, M., Garnish, J.D., Hutton, V.R.S., Staroste, E., Wohlenberg, J., 1989. An integrated model for the geothermal field of Milos from geophysical experiments. Geothermics 18, 611–621.

Fytikas, M., Vougioukalakis, G., Lütat, U., 1995. I.G.C.P. 3rd Annual Meeting Pre-Meeting Field Trip to Milos September 15–17, 1995 Guidebook, 74 pp.

Galanopoulos, V., Koinakis, I., 1991. The hydrothermal mineralization (Mn–Ba–Fe–Si) of the public mine in Vani area—Milos. Institute of Geology and Mineral Exploration (I.G.M.E.) Special Publication, 54 pp. (In Greek).

Galanopoulos, D., Hutton, V.R.S., Dawes, G.J.K., 1991. The Milos geothermal field: modelling and interpretation of electromagnetic induction studies. Phys. Earth Planet. Inter. 66, 76–91.

Glasby, G.P., 1998. The relation between earthquakes, faulting and submarine hydrothermal mineralization. Mar. Georesourc. Geotechnol. 16, 145–175.

Glasby, G.P., 2000. Manganese: predominant role of nodules and crust. In: Schulz, H.D., Zabel, M. (Eds.), Marine Geochemistry. Springer-Verlag, Berlin, pp. 335–372.

Glasby, G.P., Stüben, D., Jeschke, G., Stoffers, P., Garbe-Schönberg, C.-D., 1997. A model for the formation of hydrothermal manganese crusts from the Pitcairn Island hotspot. Geochim. Cosmochim. Acta 61, 4583–4597.

Glasby, G.P., Papavassiliou, C.T., Liakopoulos, A., Galanopoulos, V., 2001. Past mining of the Vani manganese deposit, Milos Island, Greece. Proceedings of the 5th International Mining History Congress, Milos, pp. 93–105.

Haq, B.U., Hardenbol, J., Vail, P.R., 1987. Chronology of fluctuating sea levels since the Triassic. Sci. 235, 1156–1167.

Hass, J.L., 1971. The effects of salinity on the maximum thermal gradient of a hydrothermal system at hydrostatic pressure. Econ. Geol. 66, 940–946.

Hauck, M., 1984. Die Barytlagerstätten der Inselgruppe Milos/Ägäis (Griechenland). Dr. rer nat, Thesis (Universität Karlsruhe), 241 pp.

Hauck, M., 1988. Kuroko-type ore deposits on the Aegean Islands, Greece. In: Friedrich, G.M., Herzig, P.M. (Eds.), Base Metal Sulfide Deposits. Springer Verlag, Berlin, pp. 216–228.

Hein, J.R., Schulz, M.S., Kang, J.-K., 1990. Insular and submarine ferromanganese mineralization of the Tonga–Lau region. Mar. Min. 9, 305–340.

Hein, J.R., Koschinsky, A., Halbach, P., Manheim, F.T., Bau, M., Kang, J.-K., Lubrick, N., 1997. Iron and manganese oxide mineralization in the Pacific. In: Nicholson, K., Hein, J.R., Bühn, B., Dasgupta, S. (Eds.), Manganese Mineralization: Geochemistry and Mineralogy of Terrestrial and Marine Deposits. Geol. Soc. Spec. Publ., vol. 119, pp. 123–138.

Hein, J.R., Dowling, J., Stamatakis, M.G., 1999. Hydrothermal Mn-oxide deposit rich in Ba, Zn, As, Pb and Sb′ Milos Island, Greece. In: Stanley, C.J. (Ed.), Mineral Deposits: Processes to Processing. A.A. Balkema, Rotterdam, pp. 519–522.

Hein, J.R., Stamatakis, M.G., Dowling, J. et al., 2000. Trace metal-rich Quaternary hydrothermal manganese-oxide and barite deposit, Milos Island, Greece. Trans. Inst. Min. Metall., Sect. B 109, B67–B76.

Hewett, D.F., 1964. Veins of hypogene manganese oxide minerals in the southwestern United States. Econ. Geol. 59, 1429–1472.

Hewett, D.F., 1971. Corondite—modes of occurrence and origin. Econ. Geol. 66, 164–177.

Hodkinson, R.A., Cronan, D.S., Varnavas, S., Perissoratis, C.,

1994. Regional geochemistry of sediments from the Hellenic Volcanic Arc in regard to submarine hydrothermal activity. Mar. Georesourc. Geotechnol. 12, 83–129.

Holtsam, D., Langhof, J. (Eds.), Långban The Mines, Their Minerals, Geology and Explorers. Raster Forlag and the Swedish Museum of Natural History, Stockholm, 219 pp.

I.G.M.R., 1977. Geological Map of Greece, Scale 1:25.000 Sheet Milos Island. Institute of Geological and Mining Research, Athens.

Kalogeropoulos, S., Mitropoulos, P., 1983. Geochemistry of barytes from Milos Island (Aegean Sea), Greece. N. Jb. Miner. Mh. 1, 13–21.

Karageorgis, A., Anagnostou, Ch., Sioulas, A., Chronis, G., Papathanassiou, E., 1998. Sediment geochemistry and mineralogy in Milos Bay, SW Kyklades, Aegean Sea, Greece. J. Mar. Syst. 16, 269–281.

Kelepertsis, A.E., Chatzitheodoridis, E., 1989. Dispersion halos of Mn, Pb, Ba, Cu, K, and Na in weathering products of the Vani area, Milos Island, Greece, for geochemical exploration of manganese, barite and sulfide deposits. Weathering: Vol. II, Products-Deposits-Geotechnics. Theophrastus Publications, Athens, pp. 579–602.

Kelepertsis, A., Economou, K., Skounakis, S., Porfyris, S., 1990. Mineral and chemical composition of kaolins from Milos Island, Greece – procedure of kaolinite enrichment. Appl. Clay Sci. 5, 277–293.

Kelepertzis, A.E., Kyriakopoulos, K.G., 1991. Mineralogy and geochemistry of Mn-mineralization from Vani area of Milos Island—its genesis problem. Proc. Acad. Athens 66, 107–121.

Kilias, S.P., Naden, J., Cheliotis, I., Shepherd, T.J., Constandinidou, H., Crossing, J., Simos, I., 2001. Epithermal gold mineralisation in the active Aegean Volcanic Arc: the Profitas Ilias deposit, Milos Island, Greece. Miner. Deposita 36, 32–44.

Koukouzas, N.K., Dunham, A.C., Scott, P.W., 2000. Suitability of Greek perlite for industrial applications. Trans. Inst. Min. Metall., Sect. B 109, B105–B111.

Lavelle, J.W., Cowen, J.P., Massoth, G.J., 1992. A model for the deposition of hydrothermal manganese near mid-ocean ridge crests. J. Geophys Res. 97, 7413–7427.

Le Pichon, X., Angelier, J., 1981. The Aegean Sea. Philos. Trans. R. Soc. London, Ser. A 300, 357–372.

Liakopoulos, A., 1987. Hydrothermalisme et mineralisations metallifères de l'île de Milos (Cyclades, Grèce). Mem. Sc.Terre Univ. Curie, Paris, no. 87-36, 276 pp. + 3 Annexes.

Liakopoulos, A., 1991. La genèse de bentonite de Soulias (Île de Milos, Grèce): une approche géochimique. Miner. Wealth 75, 41–49.

Liakopoulos, A., Boulegue, J., 1987. A geochemical model for the origin of geothermal fluids and the genesis of mineral deposits in Milos Island. Terra Cognita 7, 228.

Liakopoulos, A., Perseil, E.A., Boulegue, J., 1986. The manganese deposits of Cape Vani (Milos Island) and its relationship to hydrothermal activity. Program with Abstracts International South European Symposium on Exploration Geochemistry IGME-AEG 9–11 November 1986 Athens-Greece. p. 42 (Abstr.).

Liakopoulos, A., Katerinopoulos, A., Markopoulos, T., Boulegue, J., 1991. A mineralogical, petrographic and geochemical study of samples from wells in the geothermal field of Milos Island (Greece). Geothermics 20, 237–256.

Mack, E., 1977. Die Erkundung und Bewertung der Meneralvorkommen auf der Insel Milos (Griechenland). Berg-Hüttenmänn. Monatsh. 122 (2a), 48–57.

Makropoulos, K., Kouskouna, V., Karnassopoulou, A., Dando, P., Varnavas, S.P., 2000. Seismicity of the Hellenic Volcanic Arc hydrothermal system in relation to geochemical parameters. Phys. Chem. Earth (B) 25, 19–23.

Mendrinos, D., 1988. Modelling of Milos Geothermal Field in Greece, Unpubl. MEng thesis, Univ. Auckland.

Mercier, J.L., 1981. Extensional–compressional tectonics associated with the Aegean Arc: comparison with the Andean Cordillera of South Peru–North Bolivia. Philos. Trans. R. Soc. London, Ser. A 300, 337–355.

Minissale, A., Duchi, V., Kolios, N., Nocenti, M., Verrucchi, C., 1997. Chemical patterns of thermal aquifers in the volcanic islands of the Aegean Arc, Greece. Geothermics 26, 501–518.

Mitropoulos, P., Tarney, J., 1992. Significance of mineral composition variations in the Aegean Island Arc. J. Volcanol. Geotherm. Res. 51, 283–303.

Mitropoulos, P., Tarney, J., Saunders, A.D., Marsh, N.G., 1987. Petrogenesis of Cenozoic volcanic rocks from the Aegean Island Arc. J. Volcanol. Geotherm. Res. 32, 177–193.

Miura, H., Hariya, Yu., 1997. Recent manganese oxide deposits in Hokkaido, Japan. In: Nicholson, K., Hein, J.R., Bühn, B., Dasgupta, S. (Eds.), Manganese Mineralization: Geochemistry and Mineralogy of Terrestrial and Marine Deposits. Geol. Soc. Spec. Publ., vol. 119, pp. 281–299.

Papanikolaou, D., Lekkas, E., Syskakis, D., 1990. Tectonic analysis of the Milos geothermal field. Bull. Geol. Soc. Greece 24, 27–46 (In Greek with English Abstract).

Papanikolaou, D., Lekkas, E., Syskakis, D., Adamopolou, E., 1993. Correlation on neotectonic structures with the geodynamic activity in Milos during the earthquakes of March 1992. Bull. Geol. Soc. Greece 28 (3), 413–428.

Papazachos, B.C., Panagiotopoulos, D.G., 1993. Normal faults associated with the volcanic activity and deep rupture zones in the southern Aegean volcanic arc. Bull. Geol. Soc. Greece 28 (3), 243–251.

Papazachos, B.C., Kiratzi, A.A., Papadimitrou, E.E., 1993. Orientation and type of active faulting in the Aegean and the surrounding area. Bull. Geol. Soc. Greece 28 (3), 233–241.

Papazachos, B.C., Karakostas, V.G., Papazachos, C.B., Scordilis, E.M., 2000. The geometry of the Wadati–Benioff zone and lithospheric kinematics in the Hellenic arc. Tectonophysics 319, 275–300.

Pavlakis, P., 1993. The strike slip tectonic regime at southern Aegean as implied by combined marine geophysical survey. Bull. Geol. Soc. Greece 28 (3), 253–273.

Petersen, S., Herzig, P.M., Hannington, M.D., 2000. Third dimension of a presently forming VMS deposit: TAG hydrothermal mound, Mid-Atlantic Ridge, 26°N. Miner. Deposita 35, 233–259.

Pflumio, C., Boulègue, J., Liakopoulos, A., Briqueu, L., 1991. Oxygen, hydrogen, strontium isotopes in the present-day and

past geothermal systems of Milos Island (Aegean Arc). In: Pagel, M., Leroy, J.L. (Eds.), Source, Transport and Deposition of Metals. A.A. Balkema, Rotterdam, pp. 107–112.

Pflumio, C., Briqueu, L., Boulegue, J., Liakopoulos, A., 1993. Geochemical and isotopic characteristics of present day and past geothermal systems of Milos Island (Aegean Arc). Resource Geology Special Issue (Proceedings of the 29th International Geological Congress 1992) 16, 53–59.

Plimer, I., 2000. Milos Geological History. KOAN Publishing House, Athens, 262 pp.

Post, J.E., 1992. Crystal structure of manganese oxide minerals. Catena, (Suppl. 21), 51–73.

Post, J.E., 1999. Manganese oxide minerals: crystal structures and economic and environmental significance. Proc. Natl. Acad. Sci. U. S. A. 96, 3447–3454.

Rahders, E., Halbach, P., Varnavas, S.P., 1999. Composition and chemistry of recent hydrothermal iron mineralizations at Yali, Greece. In: Stanley, C.J. (Ed.), Mineral Deposits: Processes to Processing. A.A. Balkema, Rotterdam, pp. 573–576.

Rey, J., Somoza, L., Martínez-Frías, J., Benito, R., Martín-Alfageme, S. et al., 1997. Deception Island (Antarctica): a new target for Fe mineralization? In: Nicholson, K., Hein, J.R., Bühn, B., Dasgupta, S. (Eds.), Manganese Mineralization: Geochemistry and Mineralogy of Terrestrial and Marine Deposits. Geol. Soc. Spec. Publ., vol. 119, pp. 239–251.

Roy, S., 1968. Mineralogy of the different genetic types of manganese deposits. Econ. Geol. 63, 760–786.

Roy, S., 1981. Manganese Deposits. Academic Press, London, 458 pp.

Roy, S., 1992. Environments and processes of manganese deposition. Econ. Geol. 87, 1218–1236.

Roy, S., 1997. Genetic diversity of manganese deposition in the terrestrial geological record. In: Nicholson, K., Hein, J.R., Bühn, B., Dasgupta, S. (Eds.), Manganese Mineralization: Geochemistry and Mineralogy of Terrestrial and Marine Deposits. Geol. Soc. Spec. Publ., vol. 119, pp. 5–27.

Schmidt, H., 1966. Montangeologische Bearbeitung des Manganerzvorkommens von Vani auf der Kykladeninsel Milos, Unpubl. Diplom Arbeit (Univ. Leoben), 37 pp.

Scott, S.D., 1997. Submarine hydrothermal systems and deposits. In: Barnes, H.L. (Ed.), Geochemistry of Hydrothermal Ore Deposits. 3rd edn. Wiley, NY, pp. 797–875.

Spartali, E., 1994. Current exploration for epithermal gold mineralisation in Post-Tertiary volcanic rocks, Milos Island, Greece. Unpubl. MSc thesis (Imperial College, London), 141 pp.

Stamatakis, M.G., Lutat, U., Regueiro, M., Calvo, J.P., 1996. Milos the mineral island. Ind. Miner. 341 (Feb.) 57, 59–61.

Stüben, D., Glasby, G.P., 1999. Geochemistry of shallow submarine hydrothermal fluids from Paleohori Bay, Milos, Aegean Sea. Exploration and Mining Geology 8, 273–287.

Usui, A., Glasby, G.P., 1998. Submarine hydrothermal manganese deposits in the Izu-Bonin-Mariana Arc: an overview. Isl. Arc 7, 422–431.

Varnavas, S.P., Cronan, D.S., 1991. Hydrothermal metallogenic processes off the islands of Nisiros and Kos in the Hellenic Arc. Mar. Geol. 99, 109–133.

Vavelidis, M., Melfos, V., 1998. Fluid inclusion evidence for the origin of the barite silver-gold-bearing Pb–Zn mineralization of the Triades area, Milos Island, Greece. Bull. Geol. Soc. Greece 32 (3), 137–144.

Wetzenstein, W., 1975. Tektonik und Metallogenese der Insel Milos/Kykladen. Bull. Geol. Soc. Greece 12, 31–39.

Zantop, H., 1978. Geological setting and genesis of iron oxides and manganese oxides in the San Francisco manganese deposit, Jalisco, Mexico. Econ. Geol. 73, 1137–1149.

Zantop, H., 1981. Trace elements in volcanogenic manganese oxides and iron oxides: the San Francisco manganese deposit, Jalisco, Mexico. Econ. Geol. 76, 545–555.